

Ultra-thin Carbon Fiber Composites: Constitutive Modeling and Applications to Deployable Structures

Lectures 5-6

Sergio Pellegrino

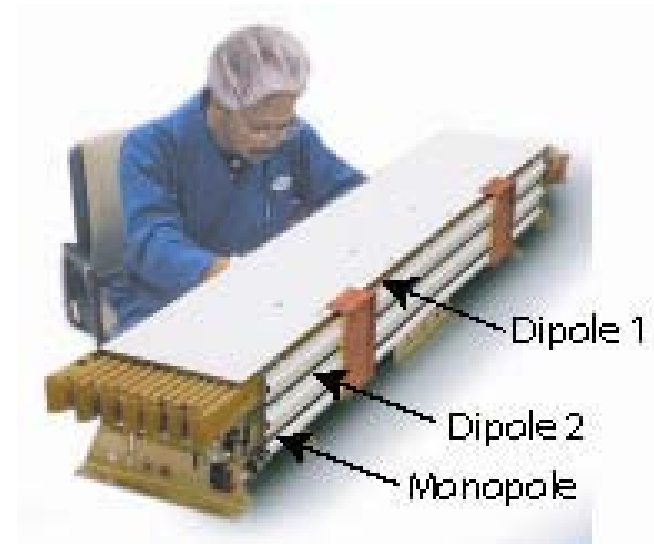
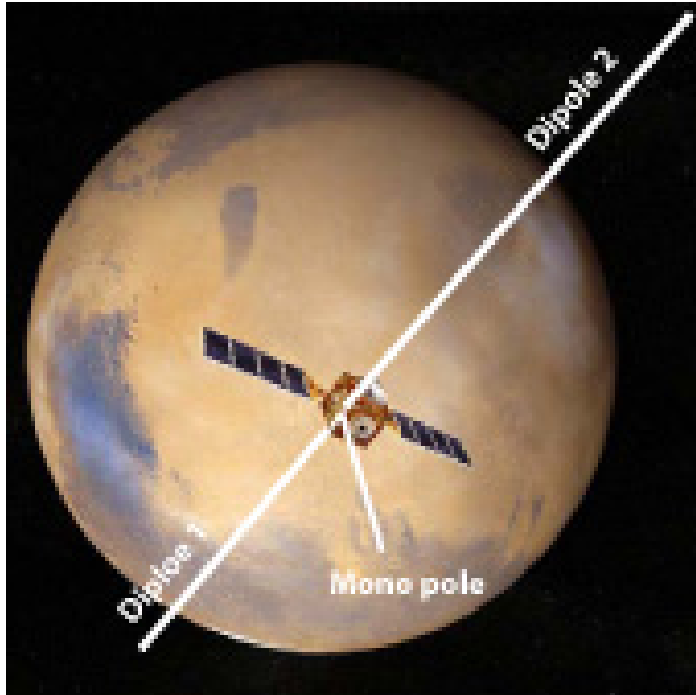
California Institute of Technology

sergiop@caltech.edu

Outline

- Further examples of ultra-thin composite deployable structures
- Tape spring hinges:
 - fabrication,
 - ABD matrix,
 - quasi-static folding and deployment experiments,
 - finite element simulations,
 - design optimization dynamic deployment,
 - finite element simulations

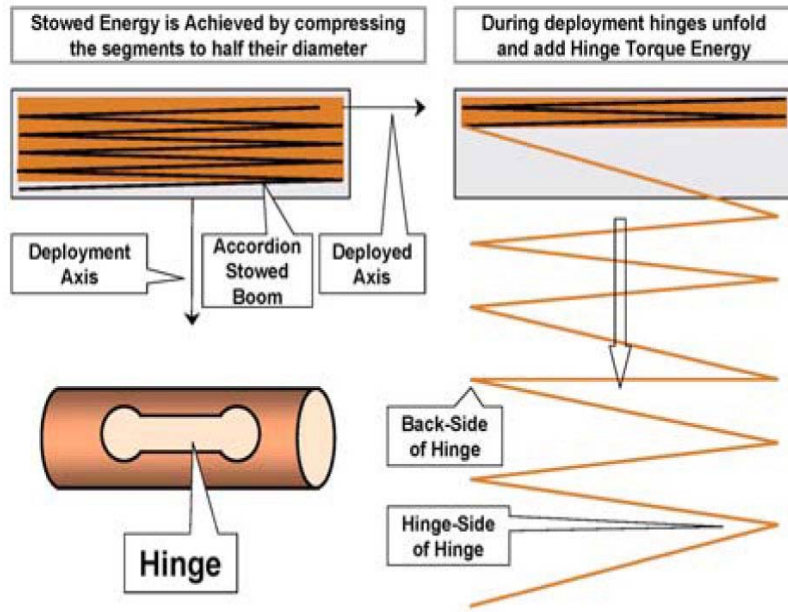
Mars Express Booms



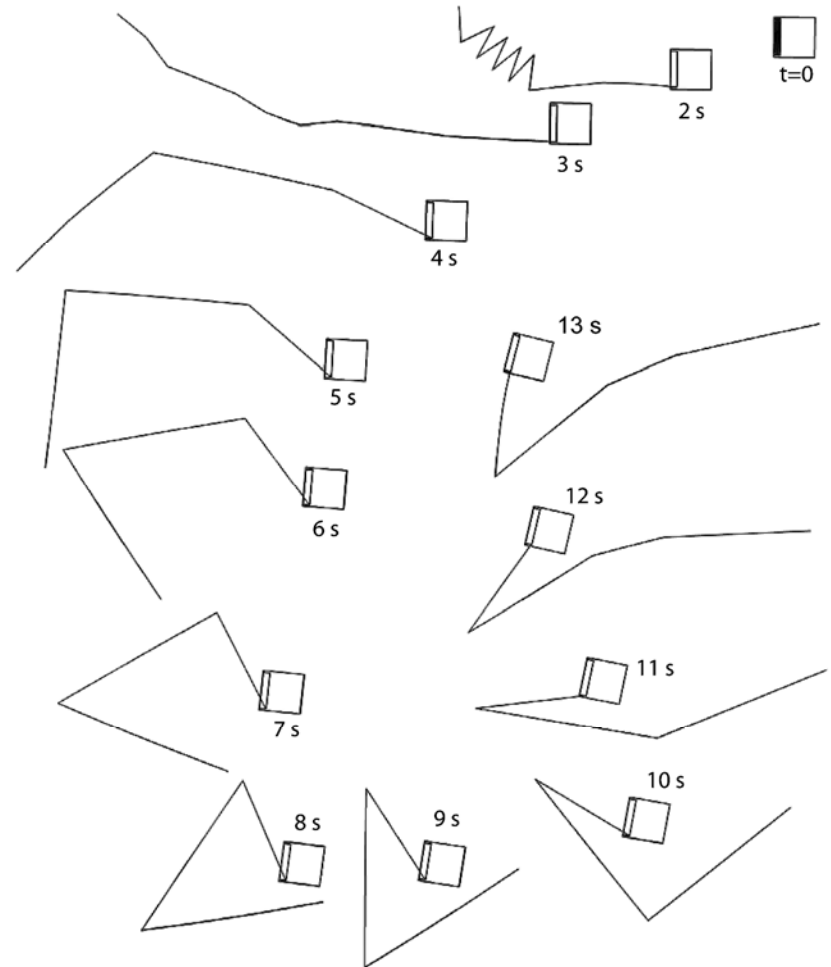
NGST Astro Aerospace Foldable
Flattenable Tubes (FFT) for MARSIS
antenna



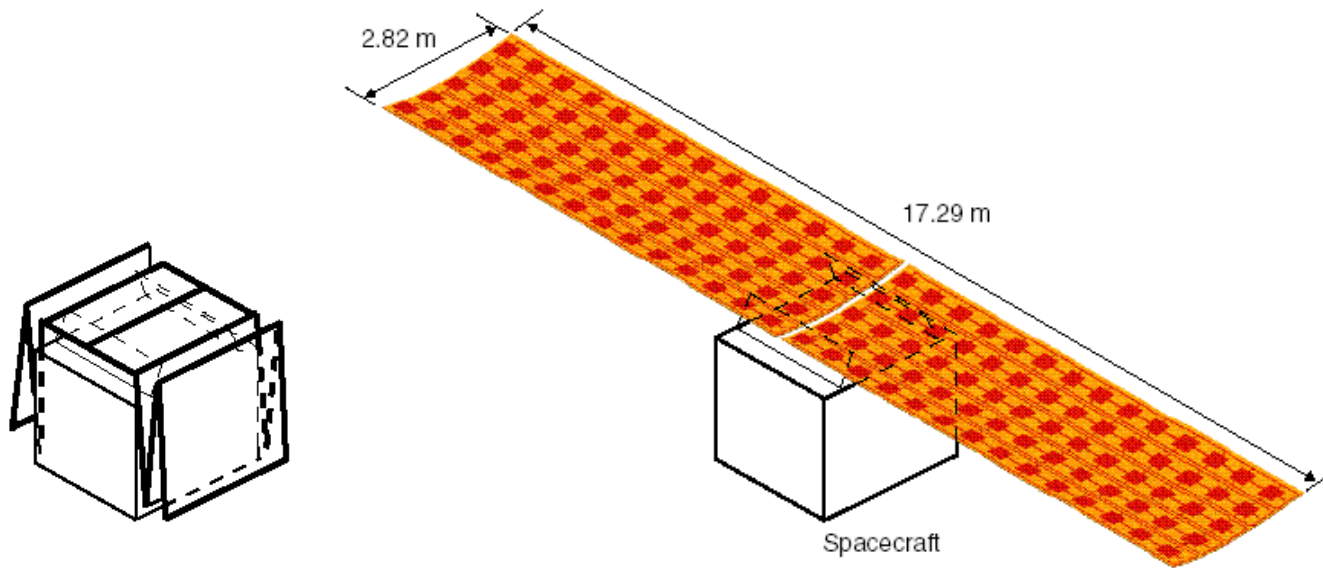
Deployment: Concept vs Actual Behaviour



(Mobrem and Adams, Analysis of the lenticular jointed MARSIS antenna deployment, AIAA-2006-1683)

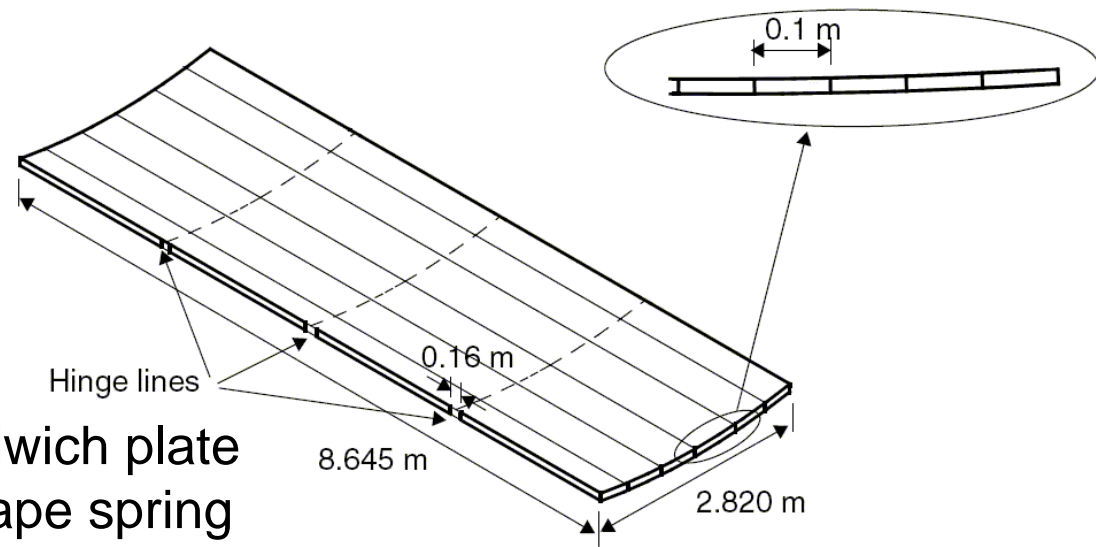


P-Band SAR (0.5 GHz)



- Monolithic array with 5-rows of 28-elements per row
- Based on Folding Large Antenna Tape Spring (FLATS) structure
- Planar beam produced by phase correction at each row power source

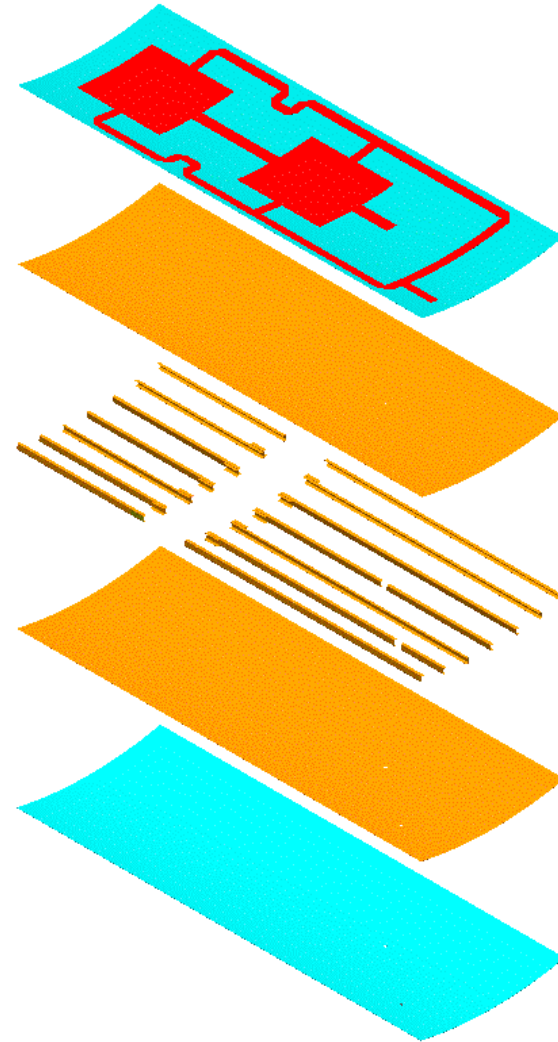
Mechanical Design



- Transversally curved sandwich plate structure forming a giant tape spring
- Chosen shape provides significant increase in stiffness, yet can be folded
- One sheet 8.64 m by 2.82 m would not be stiff enough
 - RF design requires 2 sheets @ 20 mm spacing, (signal & ground planes)
 - Classic honeycomb core replaced by longitudinal ribs @ 100 mm spacing
 - Ribs interrupted at hinge lines and face-sheets bend like a tape measure.
- Shape locks structure into place on deployment

Test-piece design: single row of two elements

- 1.563 m long by 0.564 m wide with 30 mm curvature depth
- Structure made of Kevlar and cured in autoclave
- Structure includes a hinge-line
- Etched copper circuit and ground plane added
- 2 models made, one with 4-ply and one with 3-ply skins



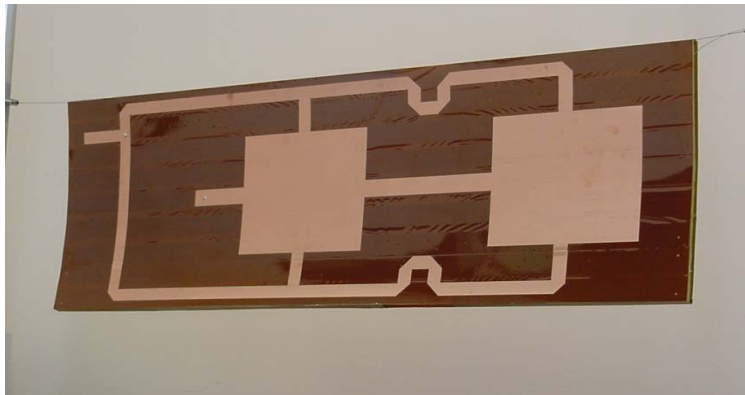
Test piece manufacturing

- Curved skins made and structure bonded together on a mould tool
- Hinge-line tested on structure
- RF circuit bonded to front skin
- Ground plane bonded to rear surface and RF connections made.



Mass 1.13 kg/m²

Accuracy ± 0.5 mm over
95% of surface



Collapsible Large Antenna Structure (CLAS) Reflector



1/10th scale model



Soykasap, Watt and Pellegrino (2005)
New concept for ultra-thin deployable
structures, Journal of IASS, 46(147): 3-8.

Tape Spring Hinges

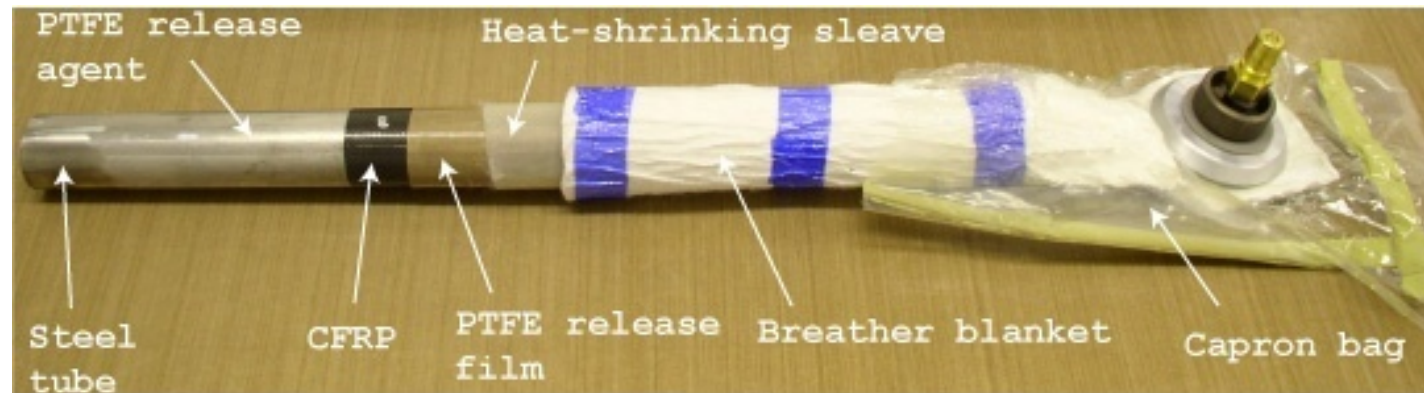
Tape Spring Hinge



- Simple but challenging
 - significant geometric non-linearities
 - symmetry breaking behaviour
- Plain weave CFRP
 - appropriate constitutive model

Construction

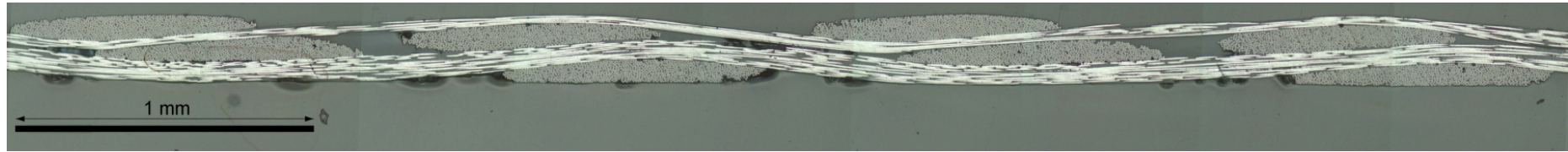
- T300-1k plain weave fabric
- Hexcel 913 epoxy resin
- Two plies at +/-45°
- 38 mm internal diameter
- Curing cycle
 - 1 hour at 125°C and 600 KPa



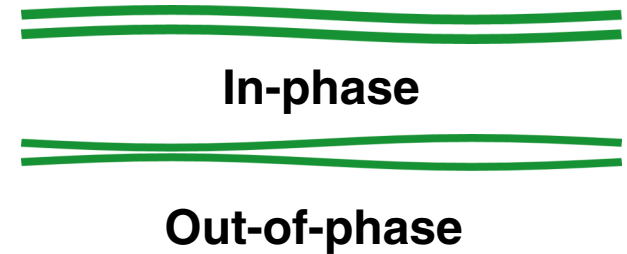
- Slotted with pressurised water jet / Dremel tool



Two Ply Plain Weave: Tow Properties

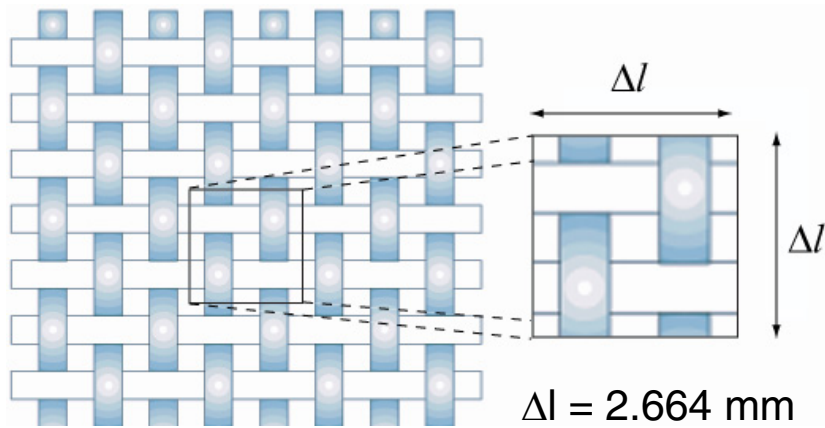


- Fibre volume fraction = 0.68
- Max. tow thickness = 0.059 mm
- Avg. tow area = 0.0522 mm²



T300-1k/913 tow properties	Value
Longitudinal stiffness, E_1 (N/mm ²)	159, 520
Transverse stiffness, $E_2 = E_3$ (N/mm ²)	11,660
Shear stiffness, $G_{12} = G_{13}$ (N/mm ²)	3,813
Shear stiffness, G_{23} (N/mm ²)	3,961
Poisson's ratio, $\nu_{12} = \nu_{13}$	0.27
Poisson's ratio, ν_{23}	0.47

Computation of ABD Matrix



- Repetitive unit cell
- Homogenized plate
- Periodic boundary conditions

- Translation terms

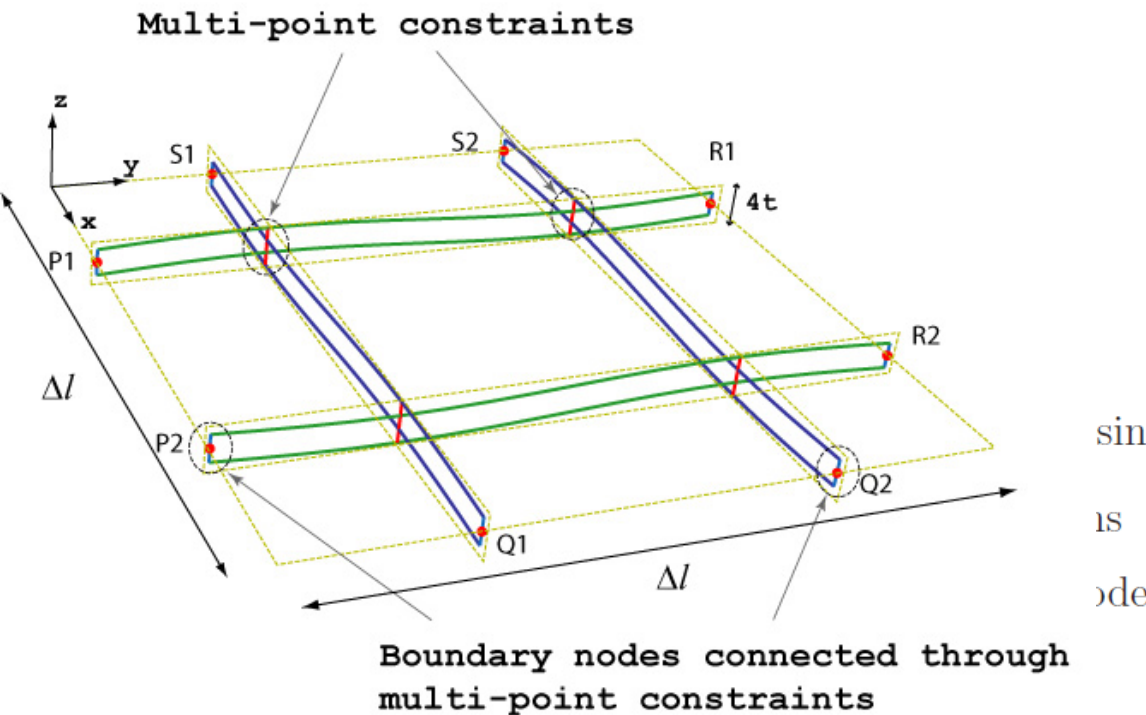
$$\Delta u_i = \overline{\varepsilon}_{ij} \cdot \Delta l$$

- Rotation terms

$$\Delta \theta_i = \overline{\kappa}_{ij} \cdot \Delta l$$

Using virtual work

- *ABD stiffness matrix*



ABD Matrix

[0/90]₂

$$\begin{Bmatrix} N_x \\ N_y \\ N_{xy} \\ \text{---} \\ M_x \\ M_y \\ M_{xy} \end{Bmatrix} = \begin{pmatrix} 13009 & 1085 & 0 & | & 0 & 0 & 0 \\ 1085 & 13009 & 0 & | & 0 & 0 & 0 \\ 0 & 0 & 667 & | & 0 & 0 & 0 \\ \text{---} & \text{---} & \text{---} & | & \text{---} & \text{---} & \text{---} \\ 0 & 0 & 0 & | & 41.3 & 1.5 & 0 \\ 0 & 0 & 0 & | & 1.5 & 41.3 & 0 \\ 0 & 0 & 0 & | & 0 & 0 & 2.3 \end{pmatrix} \begin{Bmatrix} \varepsilon_x \\ \varepsilon_y \\ \gamma_{xy} \\ \text{---} \\ \kappa_x \\ \kappa_y \\ \kappa_{xy} \end{Bmatrix}$$

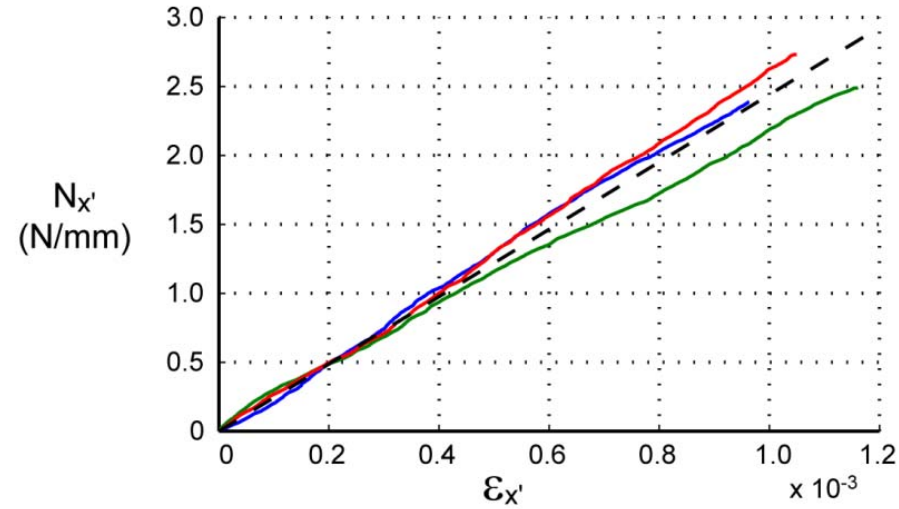
[±45]₂

$$\begin{Bmatrix} N_{x'} \\ N_{y'} \\ N_{x'y'} \\ \text{---} \\ M_{x'} \\ M_{y'} \\ M_{x'y'} \end{Bmatrix} = \begin{pmatrix} 7714 & 6380 & 0 & | & 0 & 0 & 0 \\ 6380 & 7714 & 0 & | & 0 & 0 & 0 \\ 0 & 0 & 5962 & | & 0 & 0 & 0 \\ \text{---} & \text{---} & \text{---} & | & \text{---} & \text{---} & \text{---} \\ 0 & 0 & 0 & | & 23.6 & 19.1 & 0 \\ 0 & 0 & 0 & | & 19.1 & 23.6 & 0 \\ 0 & 0 & 0 & | & 0 & 0 & 19.9 \end{pmatrix} \begin{Bmatrix} \varepsilon_{x'} \\ \varepsilon_{y'} \\ \gamma_{x'y'} \\ \text{---} \\ \kappa_{x'} \\ \kappa_{y'} \\ \kappa_{x'y'} \end{Bmatrix}$$

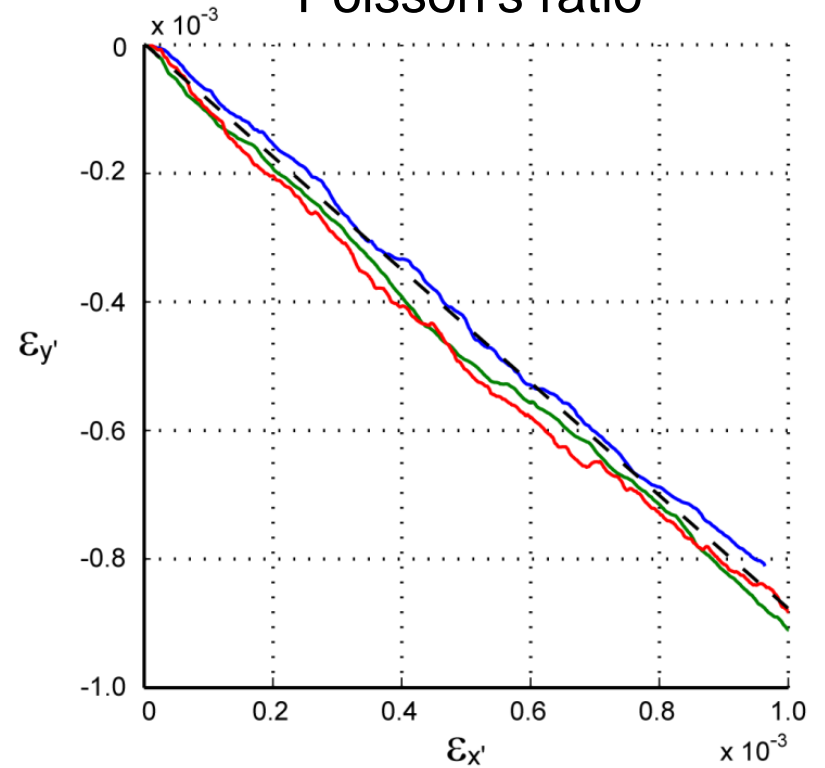
units N-mm

Experimental Validation

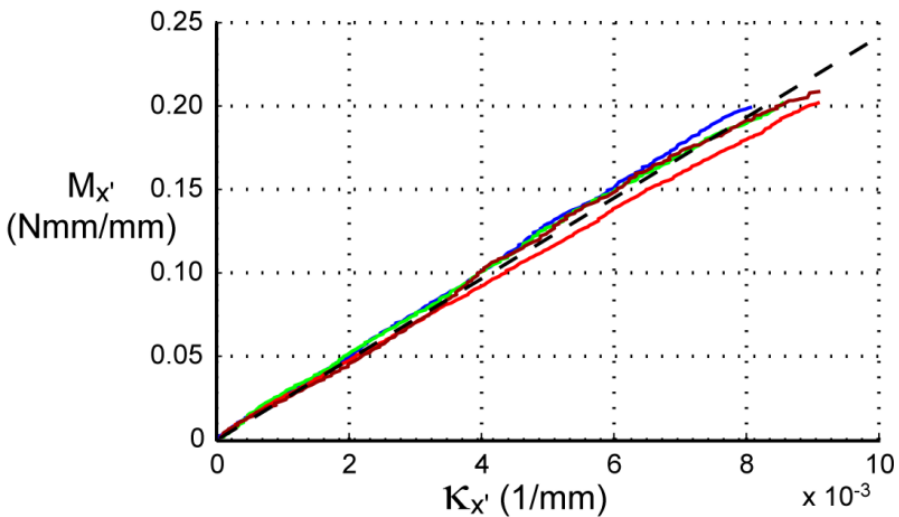
Tensile stiffness



Poisson's ratio



Bending stiffness



Note: small strains and curvatures only

Validation of ABD Matrix

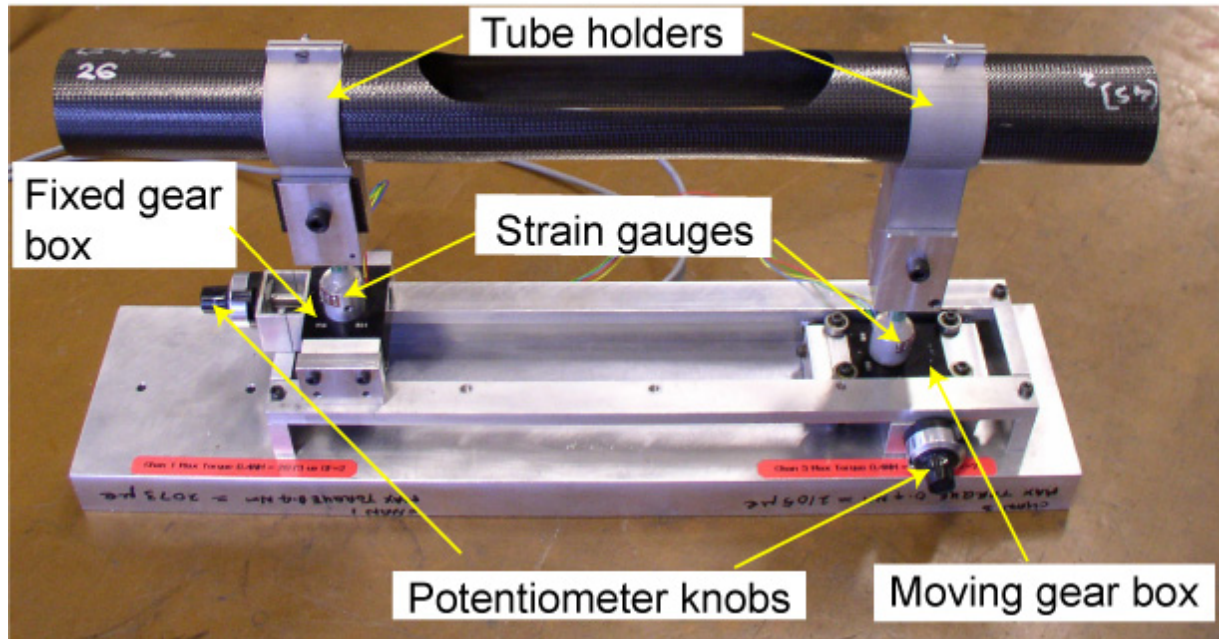
[0/90]₂

Property	Prediction	Experiment
Axial stiffness (N/mm ²)	12,108	11,898
Poisson's ratio	0.08	0.15
Bending Stiffness (Nmm)	41.3	34.5

[±45]₂

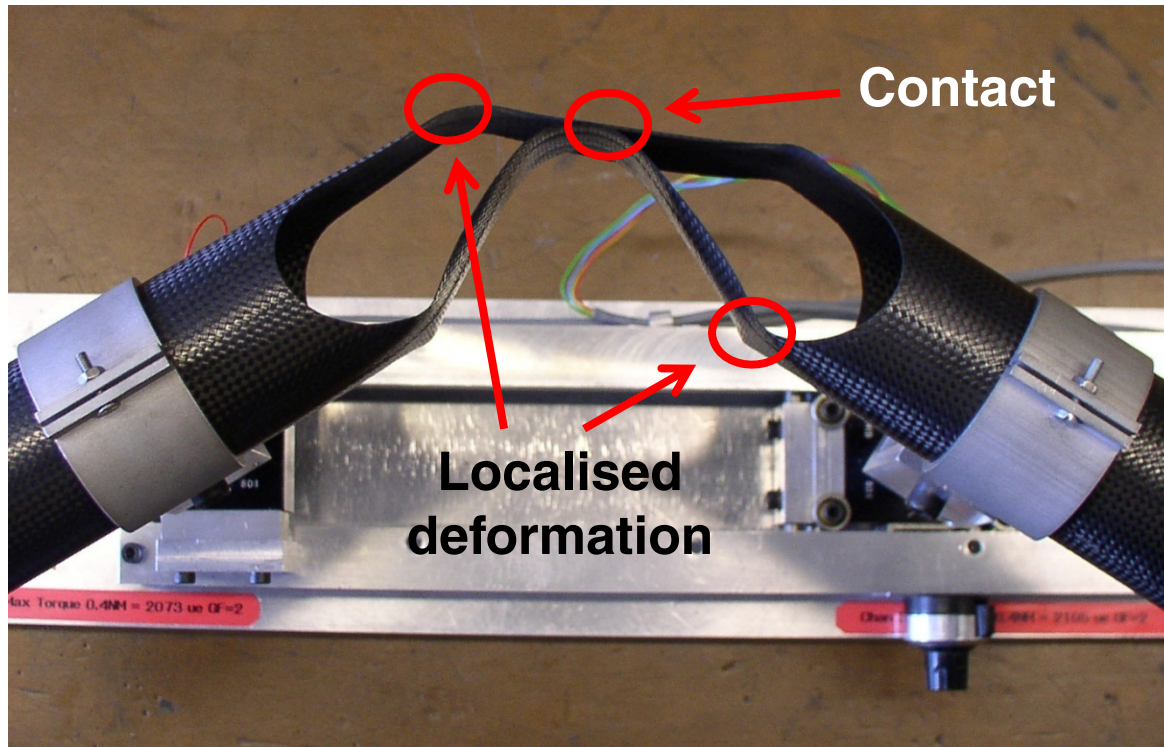
Property	Prediction	Experiment
Axial stiffness (N/mm ²)	2,437	2,440
Poisson's ratio	0.83	0.88
Bending Stiffness (Nmm)	23.6	24.2

Deployment Experiment



- Unstressed configuration
- Fold by pinching in the middle and then rotating the ends

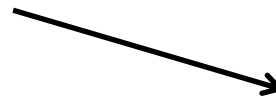
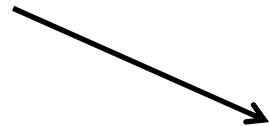
An Intermediate Configuration



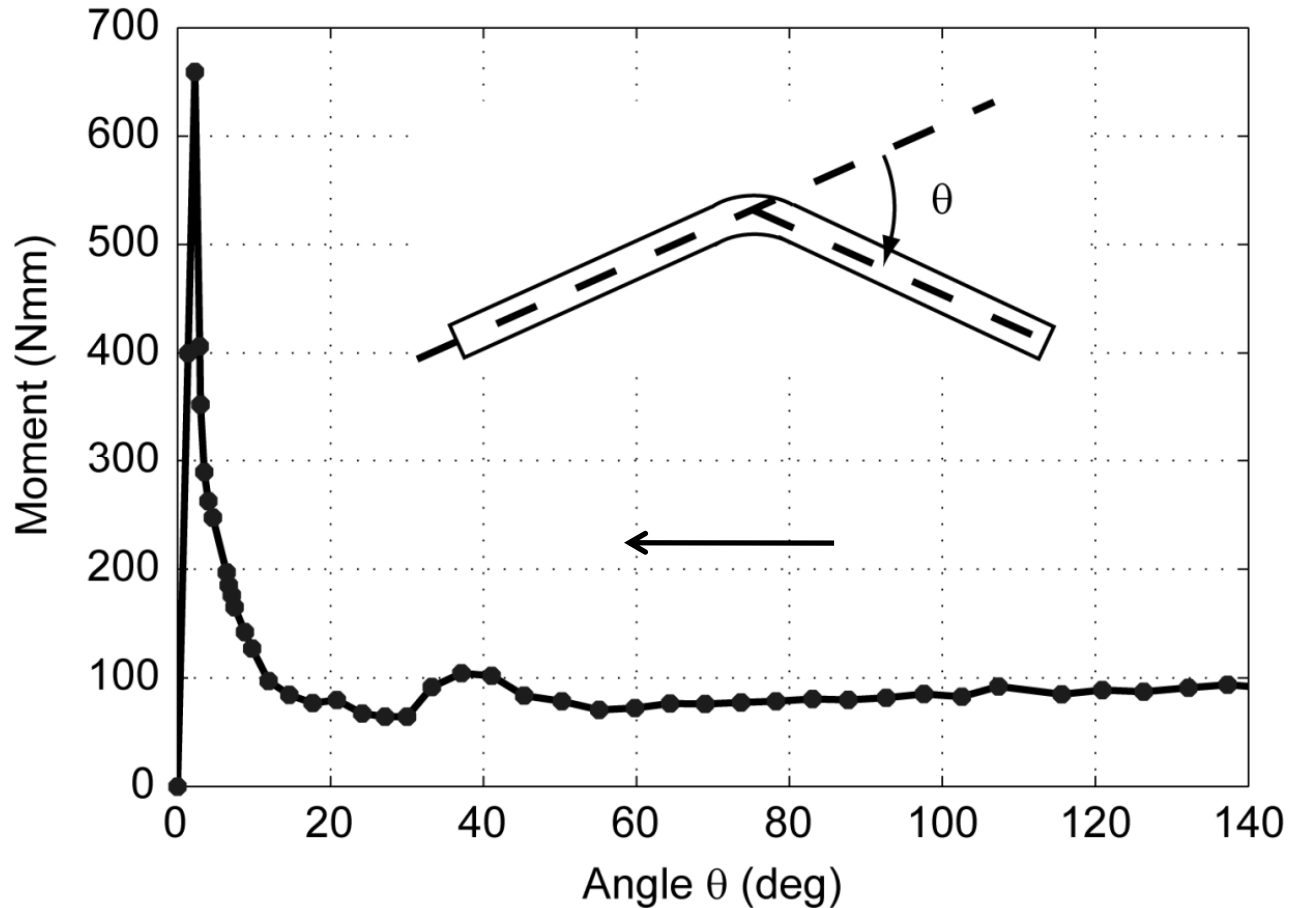
Note asymmetric folding

Quasi-Static Deployment

- Rotated back in small steps
- Equal end moments

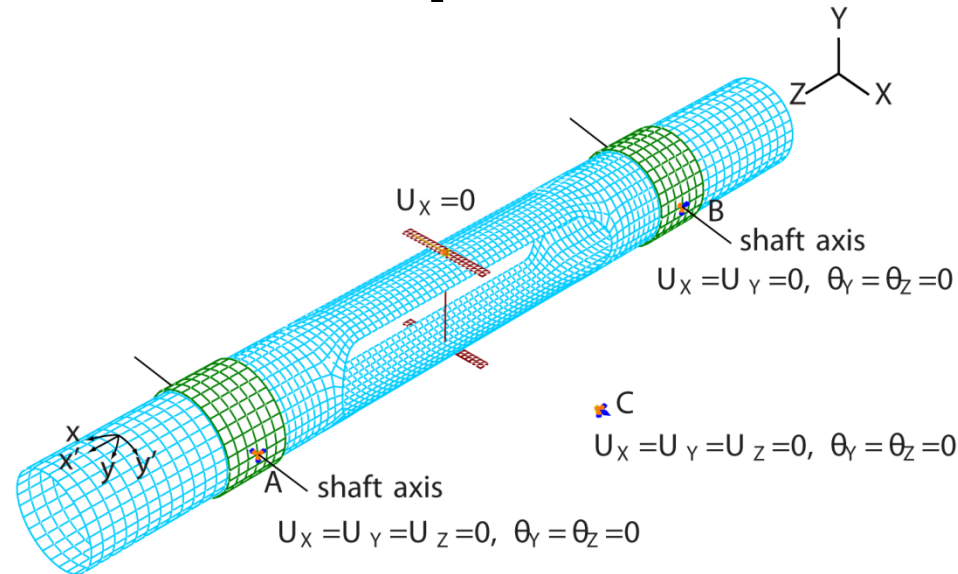


Deployment Results



- Peak moment 660 Nmm @ 2.3 deg
- Average steady state moment = 80 Nmm

ABAQUS/Explicit FE Model



- Tube modeled with 2546 nodes and 2412 shell elements (S4) minimum element length ~3 mm. Each holder modeled with 156 S4 shell elements. Nodes of holder rigidly attached nodes of tube hinge using *Tie constraints.
- Elastic properties of shell elements defined in cylindrical coordinate system x', y', z by assigning ABD' matrix with *Shell General Section parameter.
- Equal end moments simulated by attaching nodes A and B to dummy node using command *Equation. $\theta_X^A - \theta_X^B = \theta_X^C$

Three Independent Ways to Control Explicit Time Integration

- First, the integration time increment should be as large as possible, however, explicit time integration is stable only if Courant condition is satisfied (time increment cannot be larger than the time for a wave to travel between adjacent nodes). ABAQUS/Explicit estimates stable time increment limit

$$\Delta t = \alpha \left(\sqrt{1 + \xi^2} - \xi \right) \frac{L}{c_d}$$

where α is a scaling factor, L is shortest element length,

$c_d \approx \sqrt{E/\rho}$ is wave speed, ξ is fraction of critical damping in highest mode.

- Second, any loads should be applied as smoothly as possible and also the loading rate should be as high as possible.
- Third, numerical damping is used to dissipate energy build-up at high frequencies, to avoid sudden collapse of elements and generally keep the amount of kinetic energy low.

We use Two Kinds of Damping

- *Bulk viscosity* introduces in-plane strain-rate dependent pressure and in-plane curvature-rate dependent distributed moment along the edges of all shell elements.

$$p = \xi \rho c_d l \dot{\epsilon}_v \qquad p = \xi \frac{h_0^2}{12} \rho c_d L \dot{\kappa}$$

where L is a characteristic element length, h_0 the initial thickness, $\dot{\epsilon}_v$ the volumetric strain rate, $\dot{\kappa}$ twice the mean curvature rate.

- Viscous pressure introduces a velocity-dependent normal pressure on the shell $p = -c_v \mathbf{v} \cdot \mathbf{n}$

where c_v is the pressure coefficient, \mathbf{v} the velocity vector and \mathbf{n} the unit normal.

- This normal pressure is very effective in quickly damping out dynamic effects and thus reach quasi-static equilibrium in a minimal number of increments.

Remark on Mass Scaling

- This is an alternative technique that is often used to speed up explicit analyses.
- This technique consists in artificially increasing the density of the material to $\beta\rho$ in order to increase the time increment to $\beta \Delta t$
- This technique would be useful in simulations involving rate-dependent materials, where the load-rate speed-up technique adopted in the present study could not be used, but offers no advantages in the present case.

Check on Energy Histories

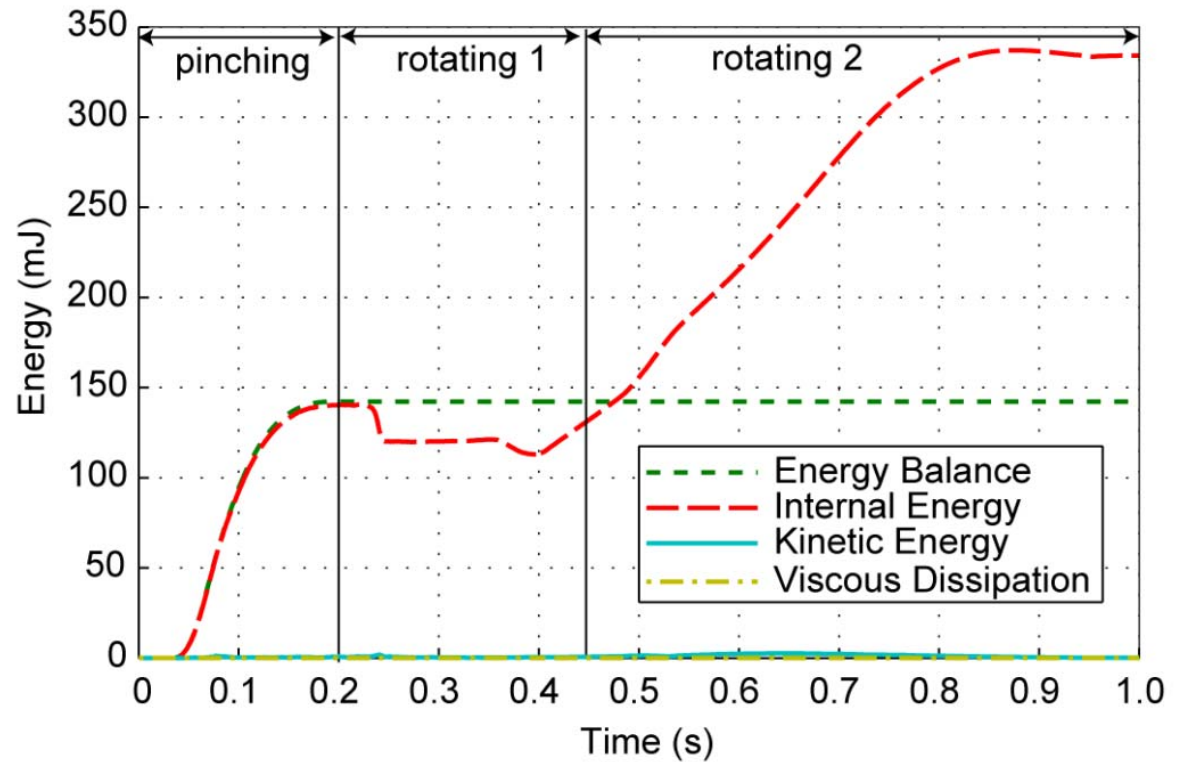
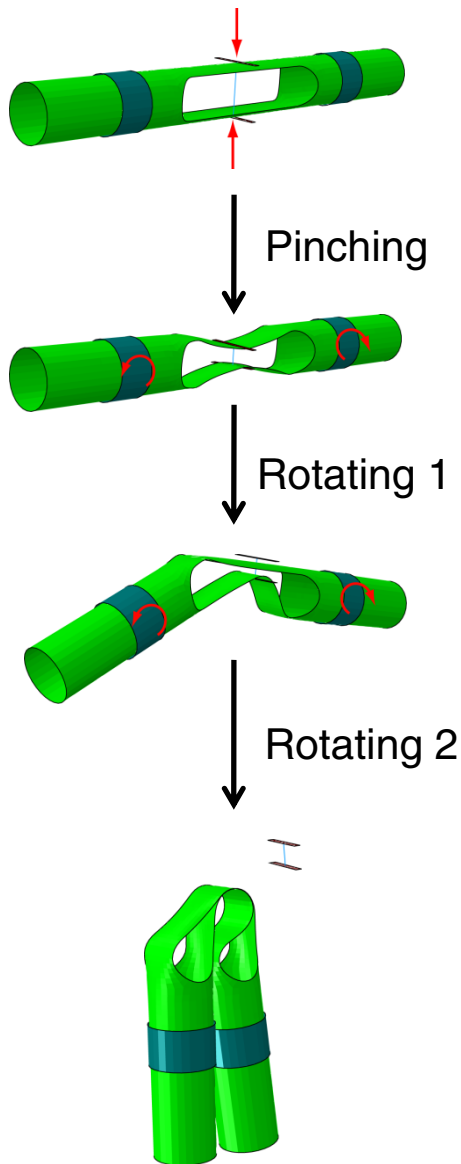
- The energy balance E_b is defined as the difference between the energy stored in the structure and/or dissipated during the loading process, $E_i + E_v + E_k$, and the work of all external forces, E_w :

$$E_b = E_i + E_v + E_k - E_w$$

where E_i is internal energy, equal to strain energy plus artificial energy (due to hourglassing), E_v is viscous dissipation, E_k is kinetic energy.

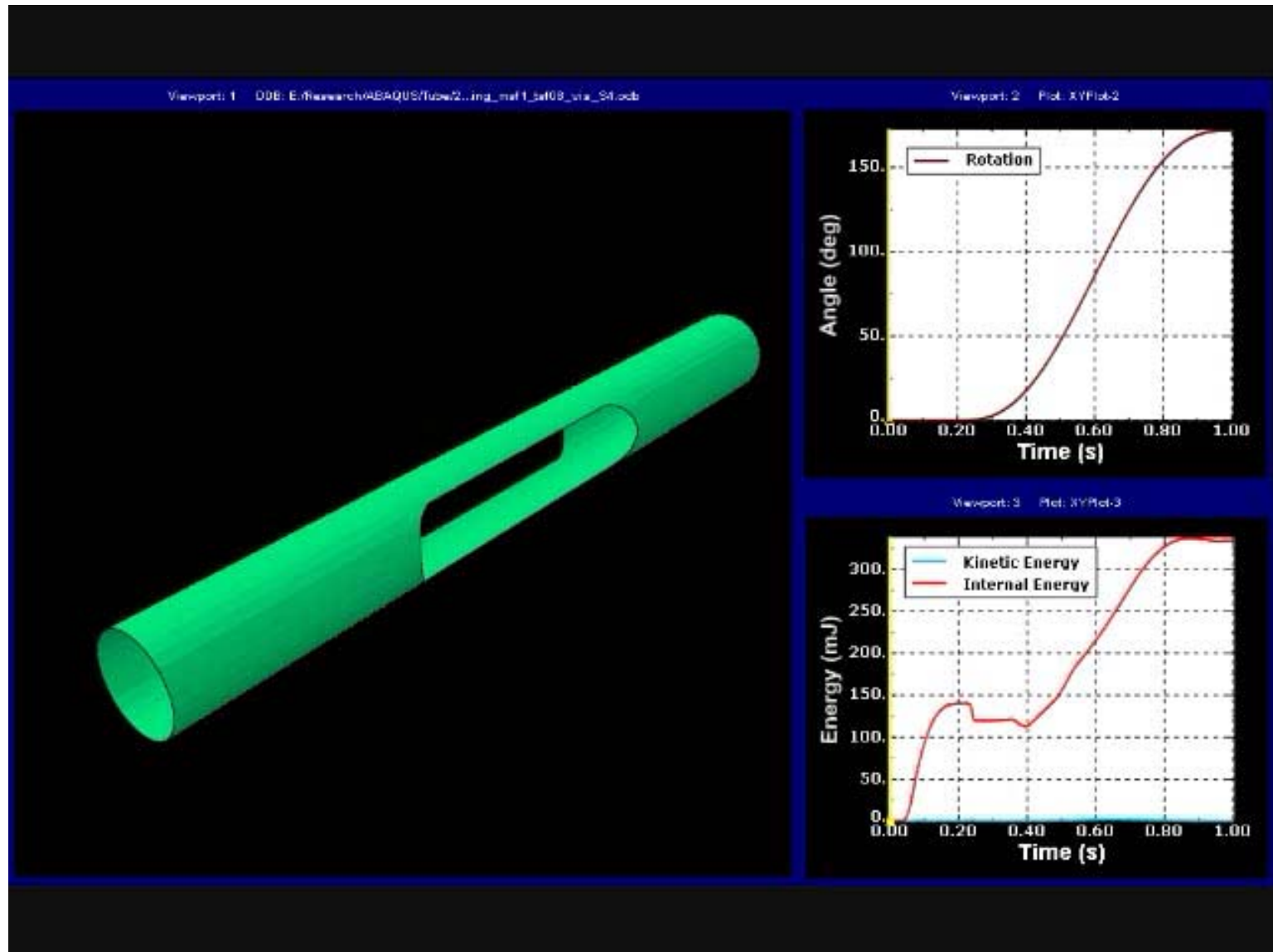
- Artificial energy was kept negligibly small by using fully integrated elements and by avoiding any localized actions on the shells.
- Two main checks on energies. First, the kinetic energy has to be a small fraction (<1%) of internal energy. Second, the energy balance should remain equal to the amount of external energy (e.g., thermal) introduced in the system.

Folding Simulation

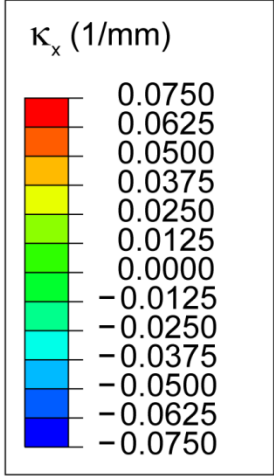
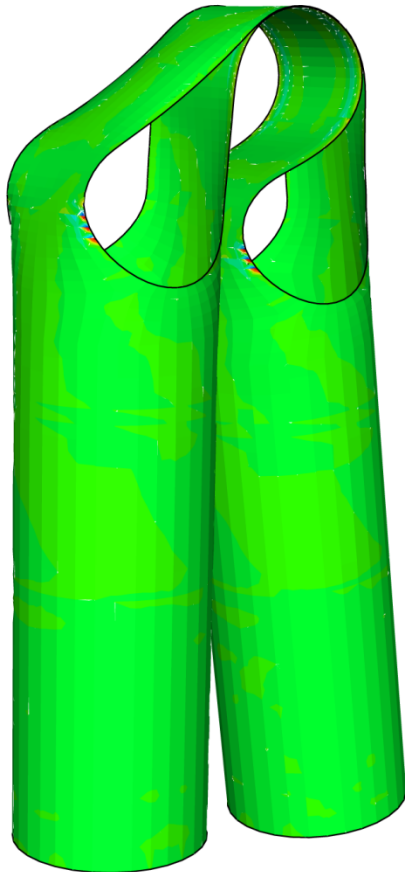
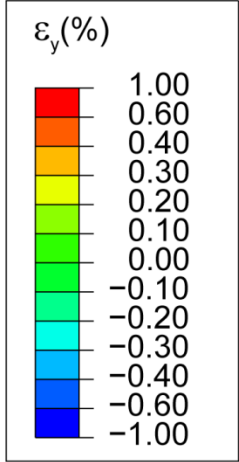


- Energy balance constant throughout rotation stages
- Thermal energy supplied to system during pinching
- Kinetic energy negligible at end of folding

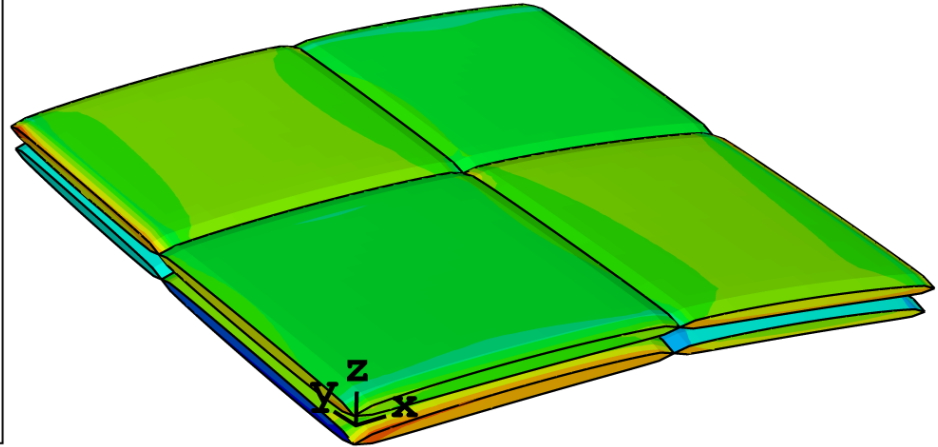
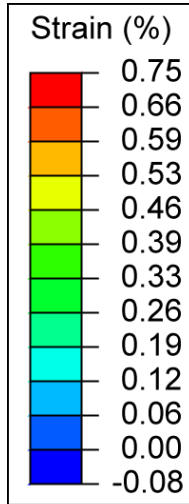
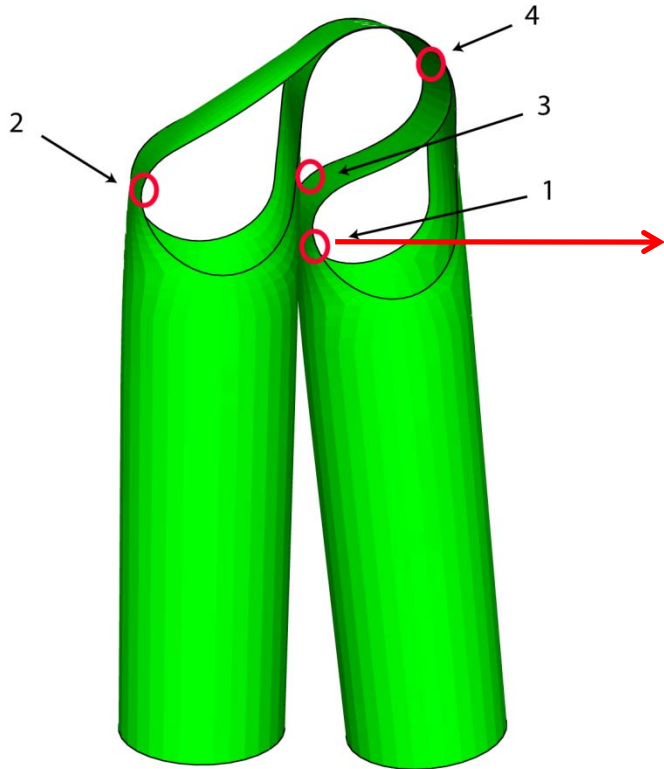
Folding Simulation



Mid-Plane Strain Variation



Failure Analysis

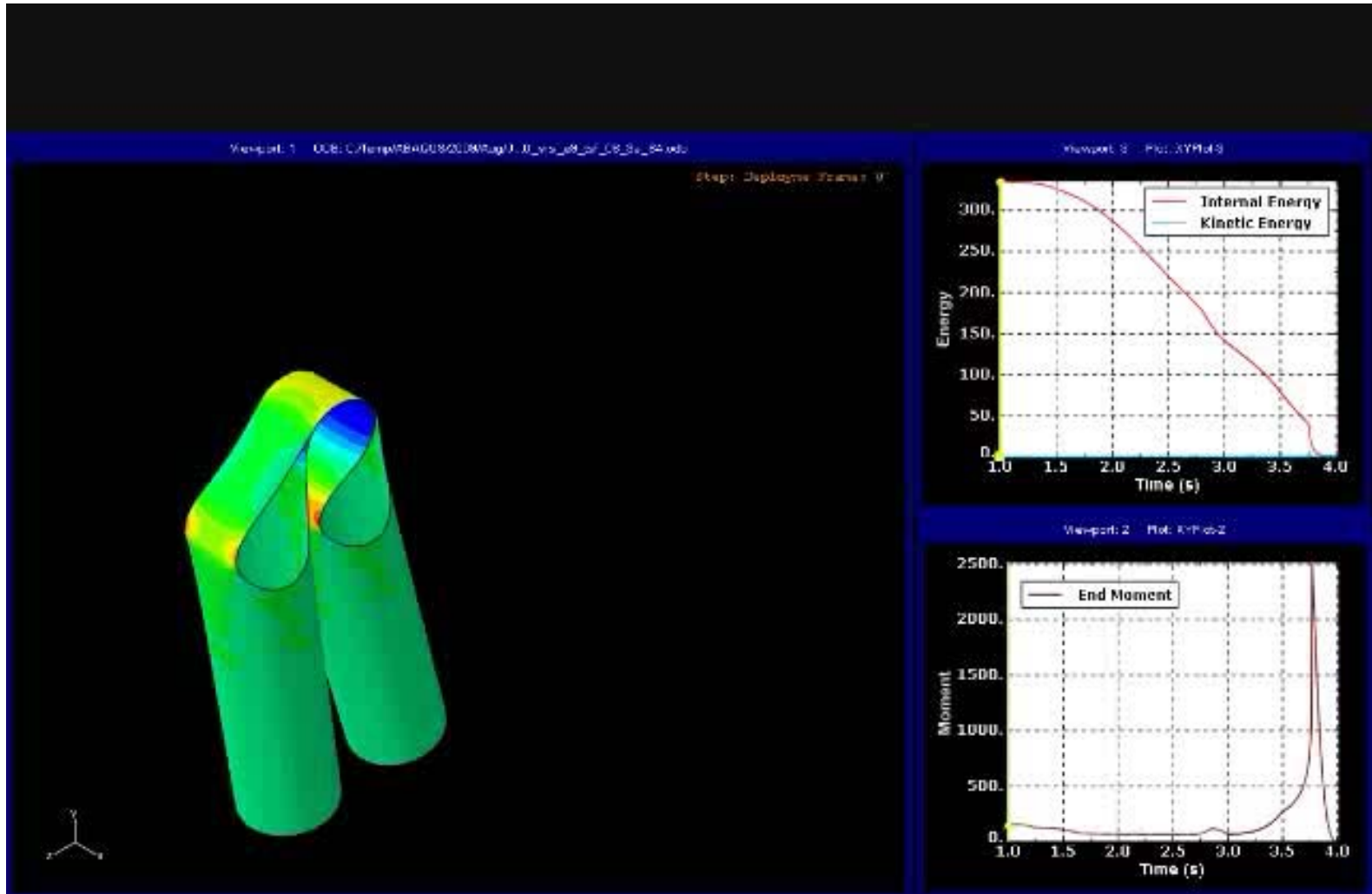


Ultimate tensile strains

- T300 fibers = 1.5%
- HexPly913 resin = 1.93%

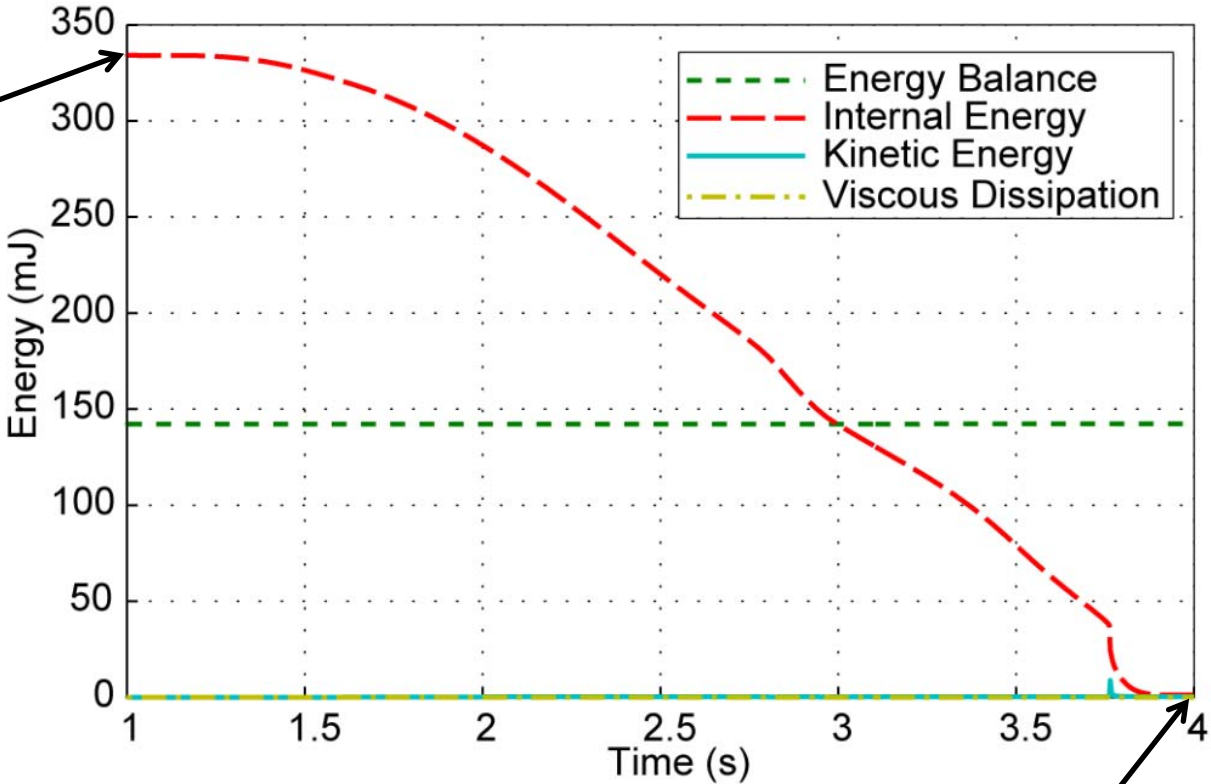
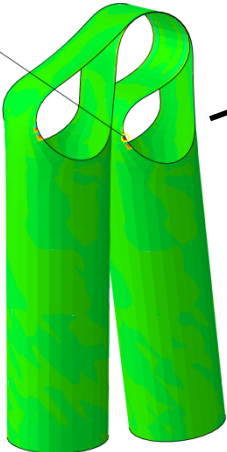
Location	1	2	3	4
Fiber (%)	0.75	0.55	0.76	0.13
Matrix (%)	1.70	1.86	1.95	0.21

Deployment Simulation

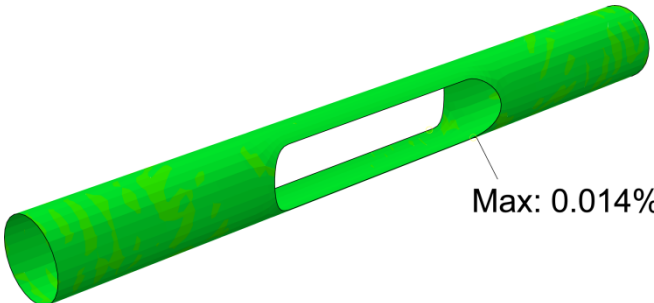


Deployment Simulation

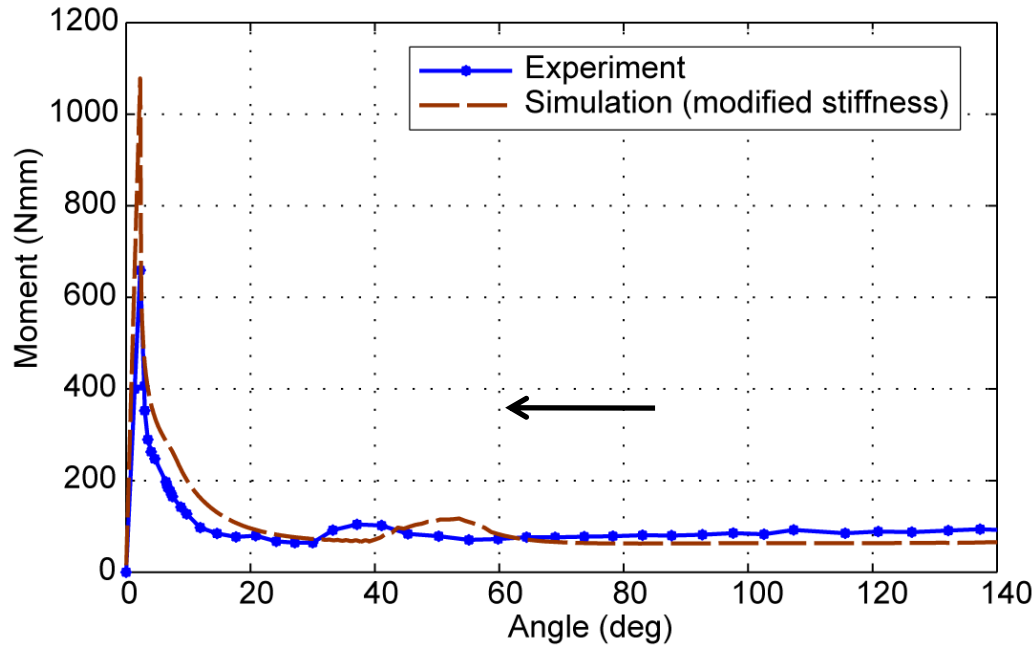
Max: 1.23%



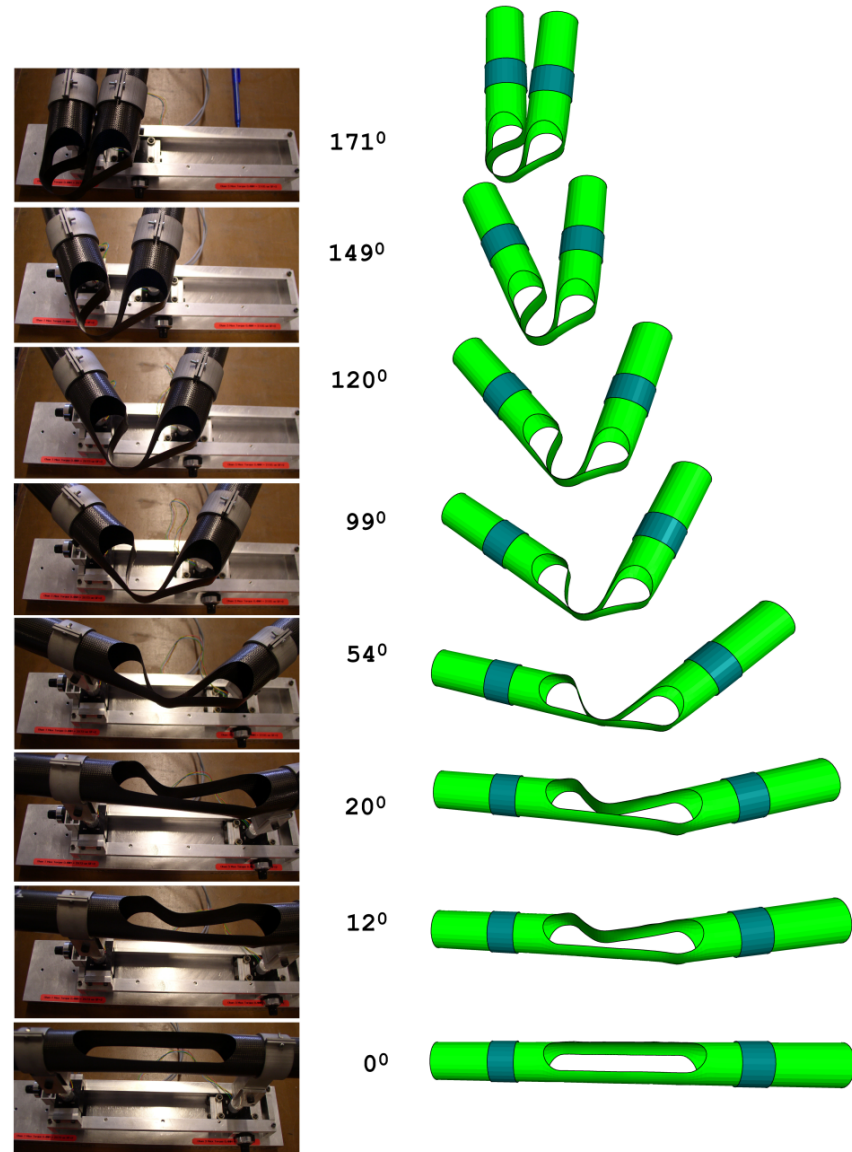
Max: 0.014%



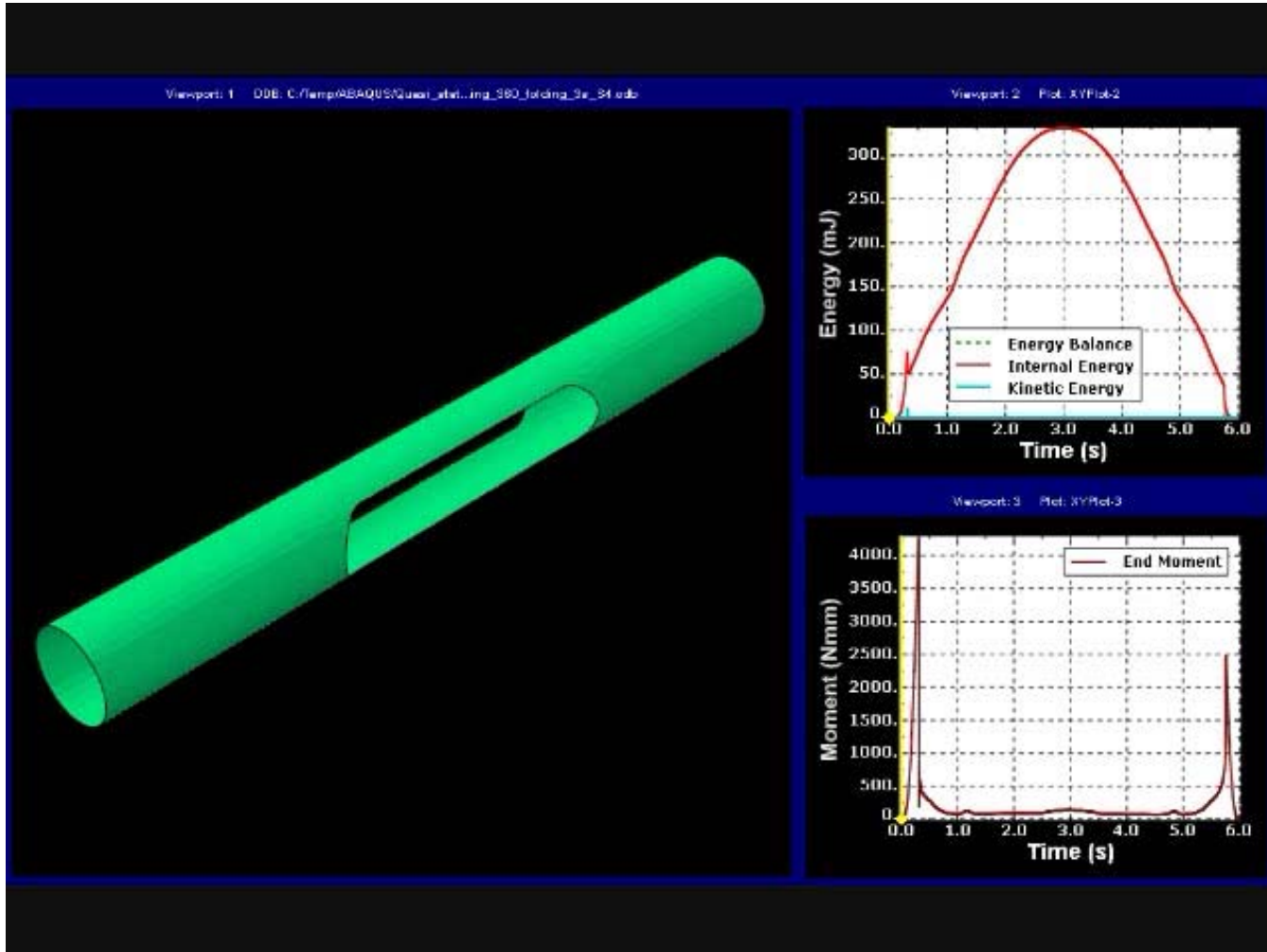
Comparison



- Good quantitative agreement for moment-rotation
- Excellent correlation in details of deformed configuration

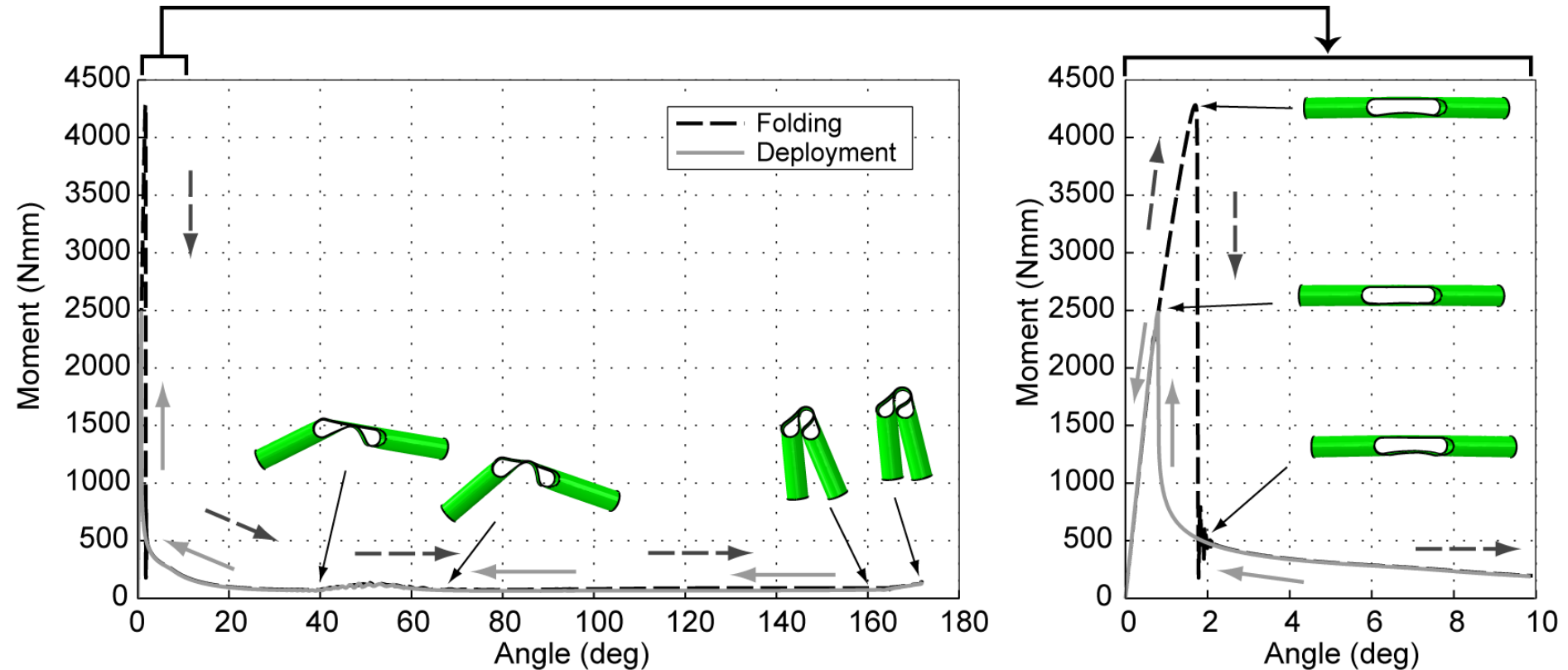


Folding and Deployment without Pinching



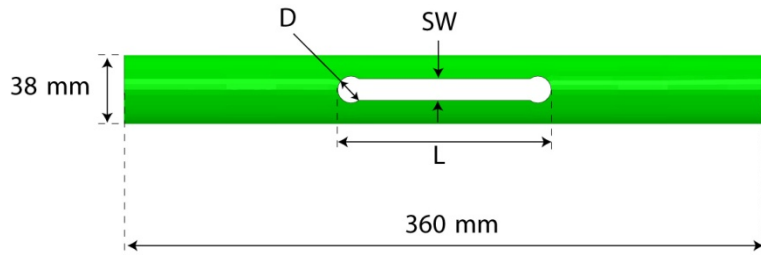
- Energy balance is constant (0 mJ)
- Kinetic energy is negligible

Moment-Rotation Relationship

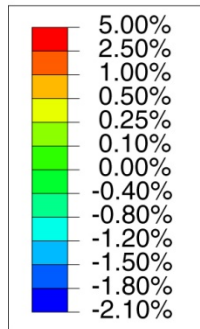


- Peaks
 - Folding: 4280 Nmm @ 1.70 deg
 - Deployment: 2482 Nmm @ 0.8 deg
- Steady state moment = 67 Nmm

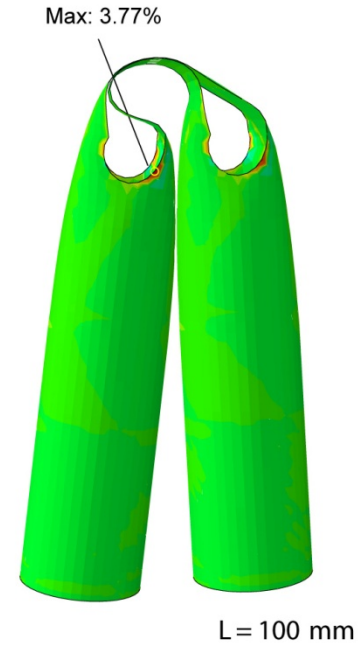
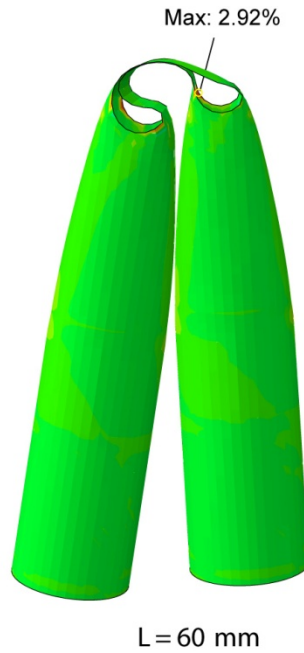
Optimization of Hinge Design



**Mid-plane strains along
+45 deg fibers**

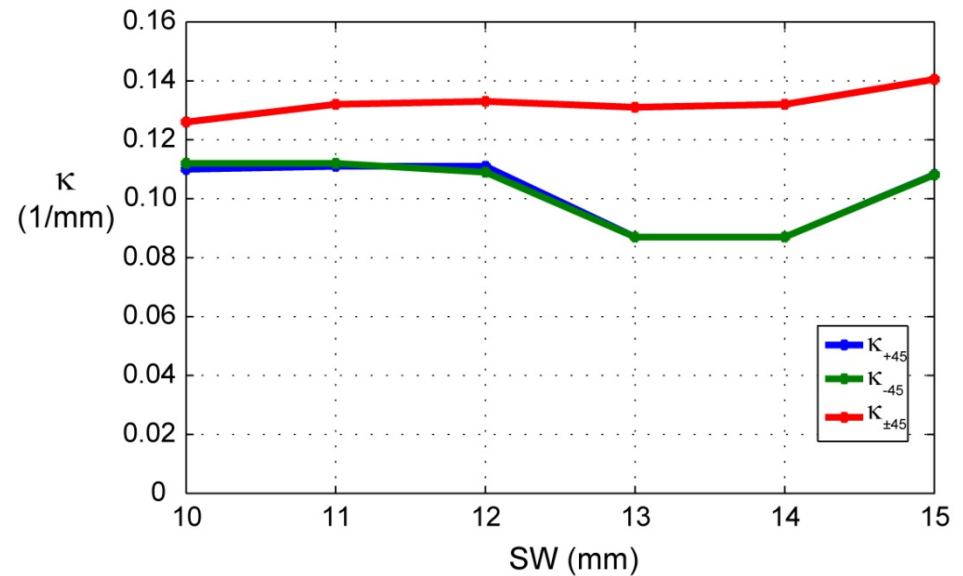
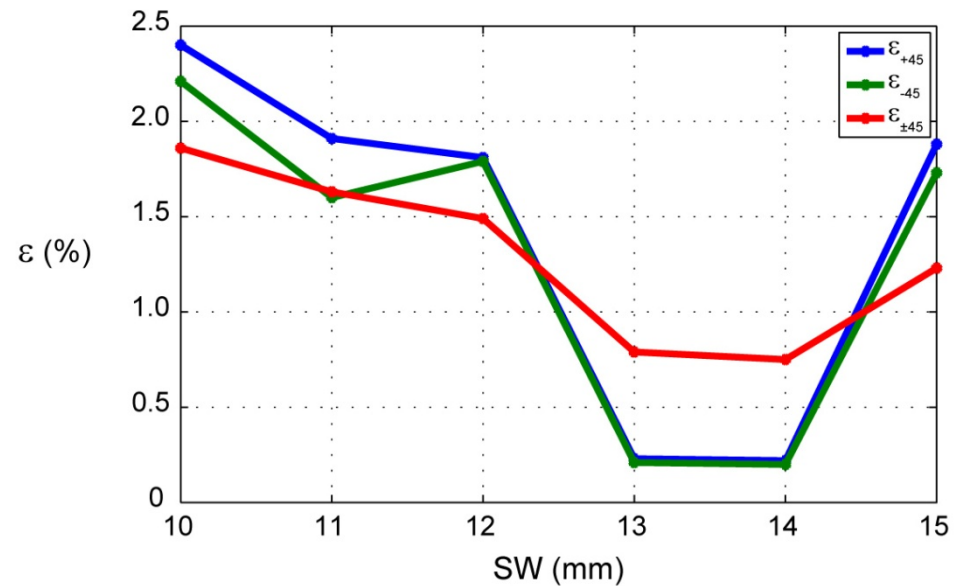


SW=10 mm
D=15mm

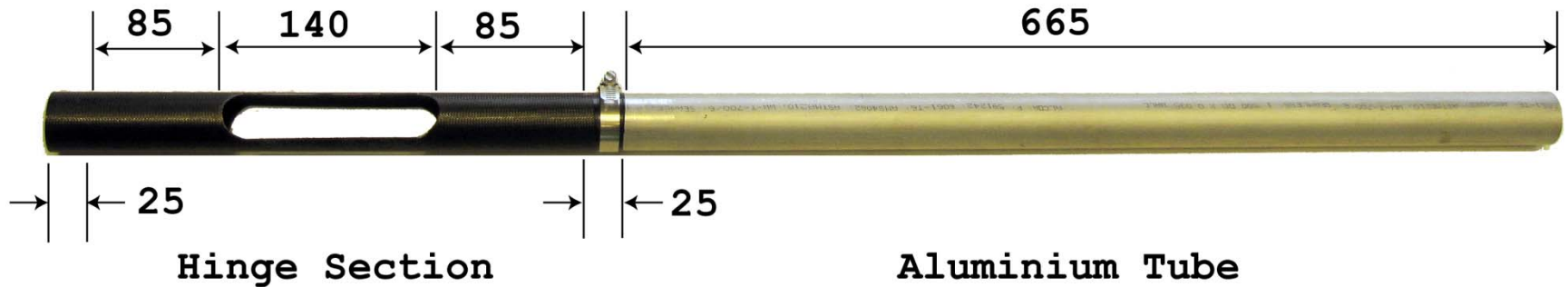


Example of Design Sensitivity

Maximum mid-plane strains
along +45 deg fibers for
D=15 mm, L=120 mm



Boom for Dynamic Deployment Test

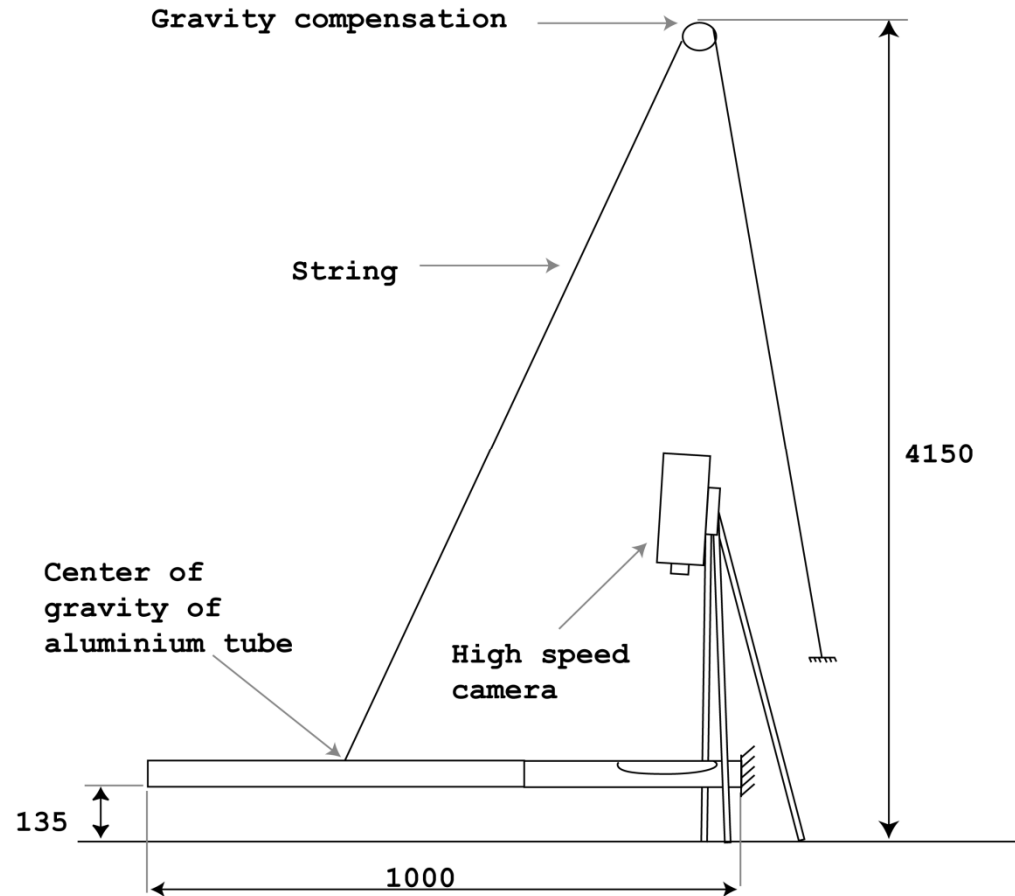


- $[\pm 45]_2$ laminate (T300-1k/Hexply913)
- 38 mm internal diameter, 0.2 mm thick
- 25 mm wide and 110 mm long straight two tape springs

- Aluminum-alloy tube
- 38 mm outer diameter, 0.9 mm thick

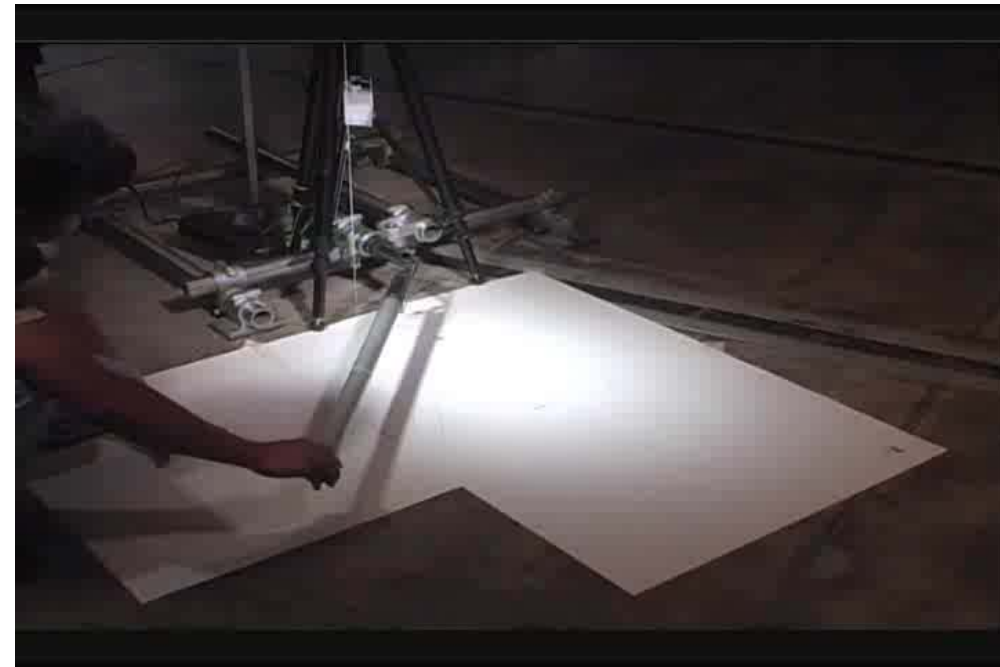
Experiment Setup

- Single-point offload allows boom to only move in horizontal plane
- High speed imaging at 300 fps
- Background with clearly marked angles
- Each test repeated on two nominally identical hinges

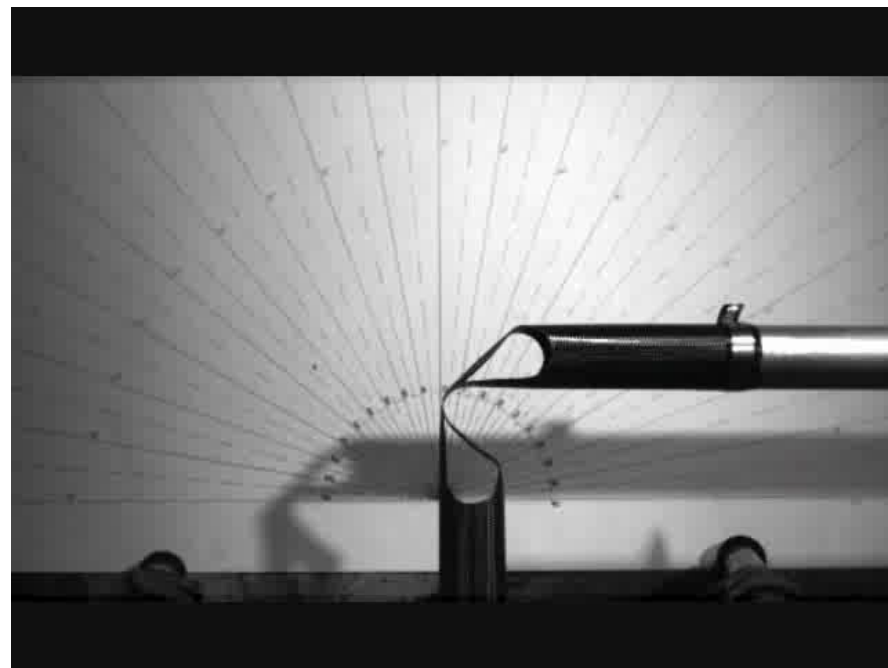


(Dimensions in mm)

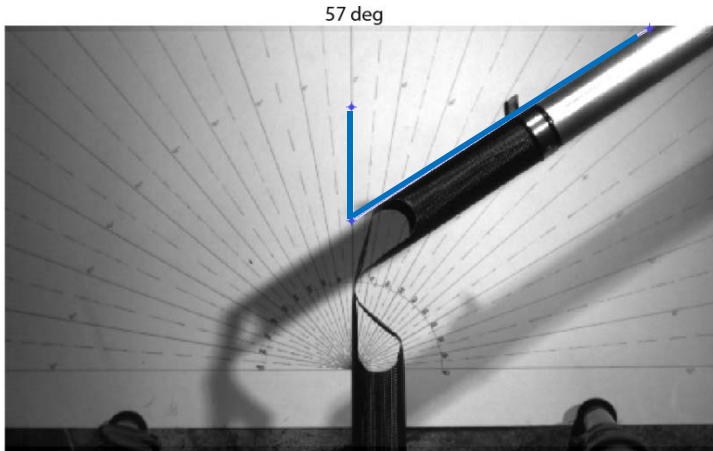
Deployment Dynamics



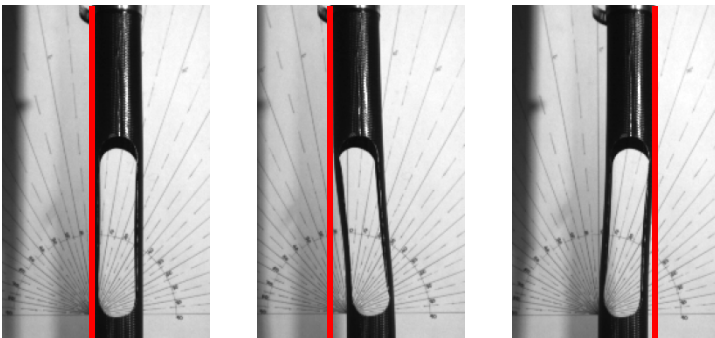
90 deg Deployment



Deployment Angle

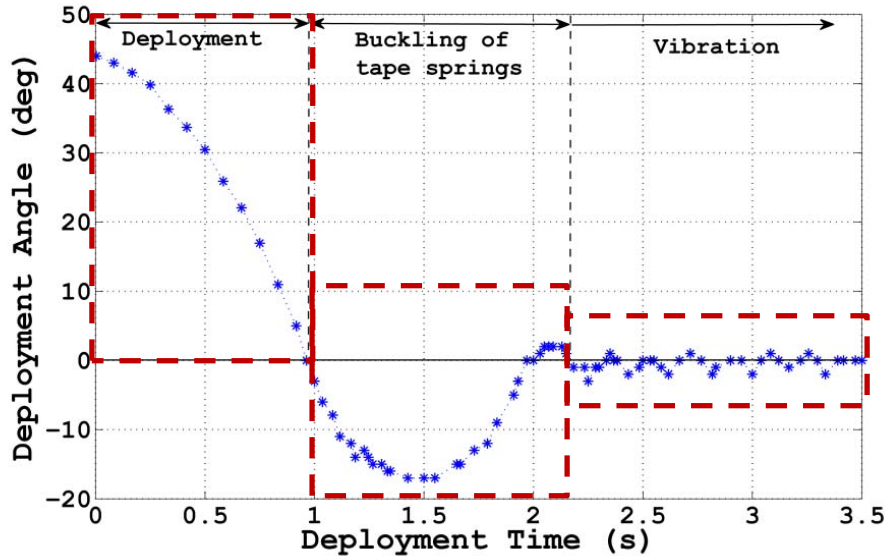


- Angle between boom and fully deployed configuration
- 1 out of every 25 frames (every 0.0083 s)
- Matlab image processing
- Hinge configuration not uniquely defined

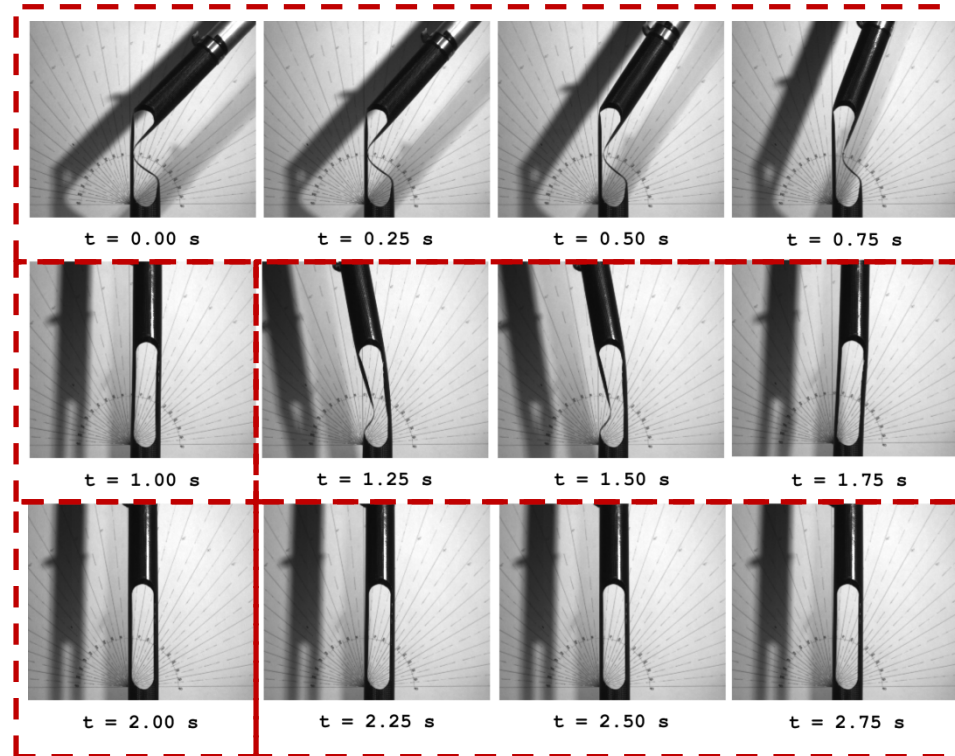


Different configurations of hinge with zero deployment angle

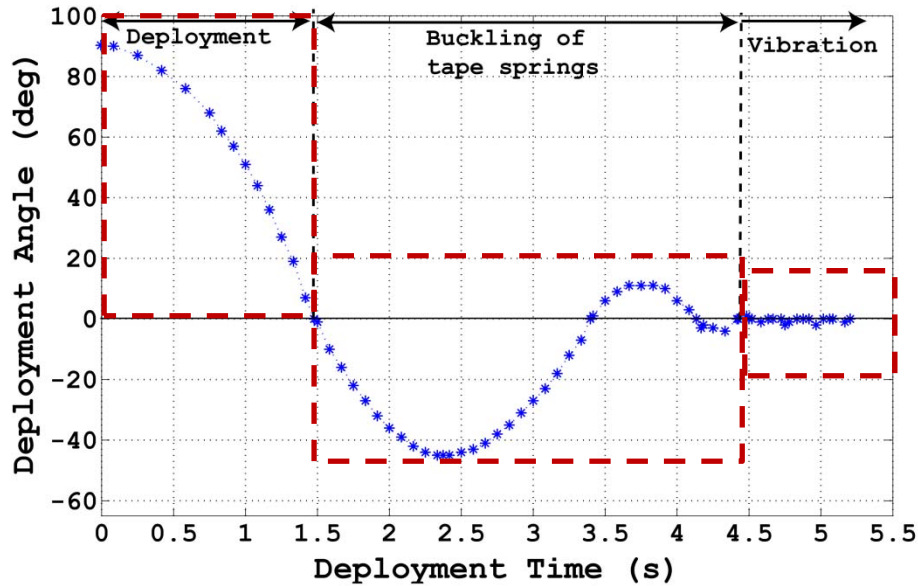
Angle vs Time (45 deg)



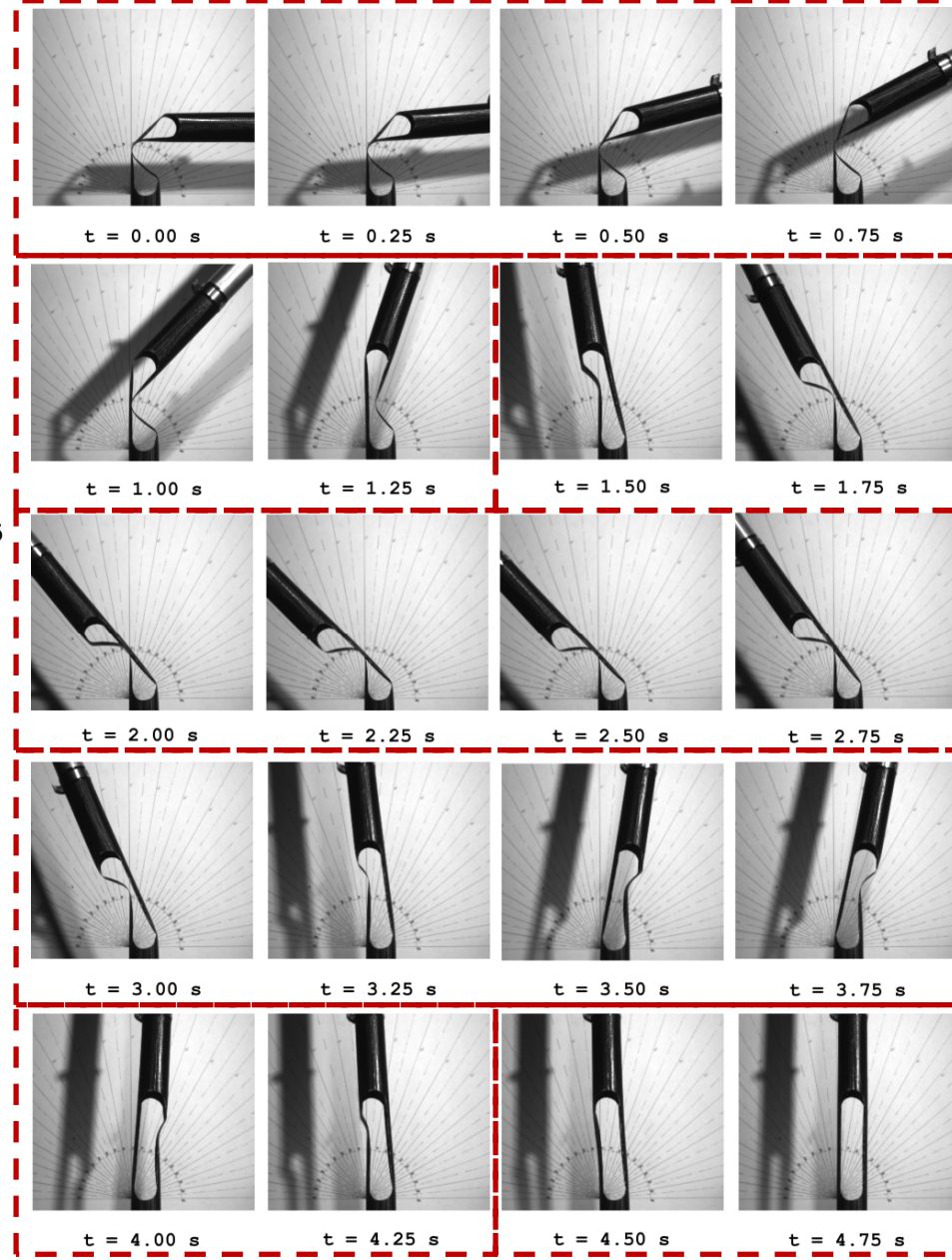
- Deployment phase: 0.96 s
- Buckling phase: 1.2 s
Maximum overshoot 17 deg
- Vibration phase: 20 s
2 deg amplitude, period 0.18 s



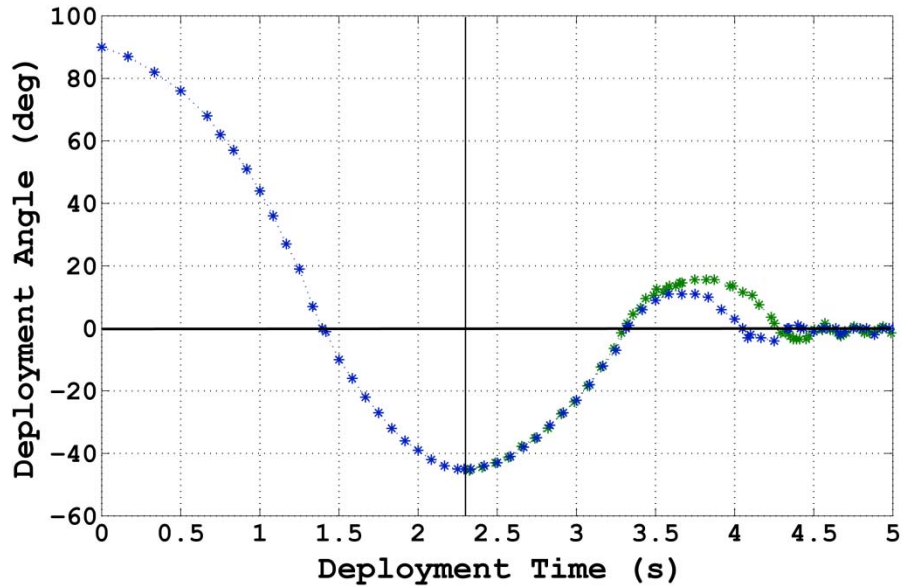
Angle vs Time (90 deg)



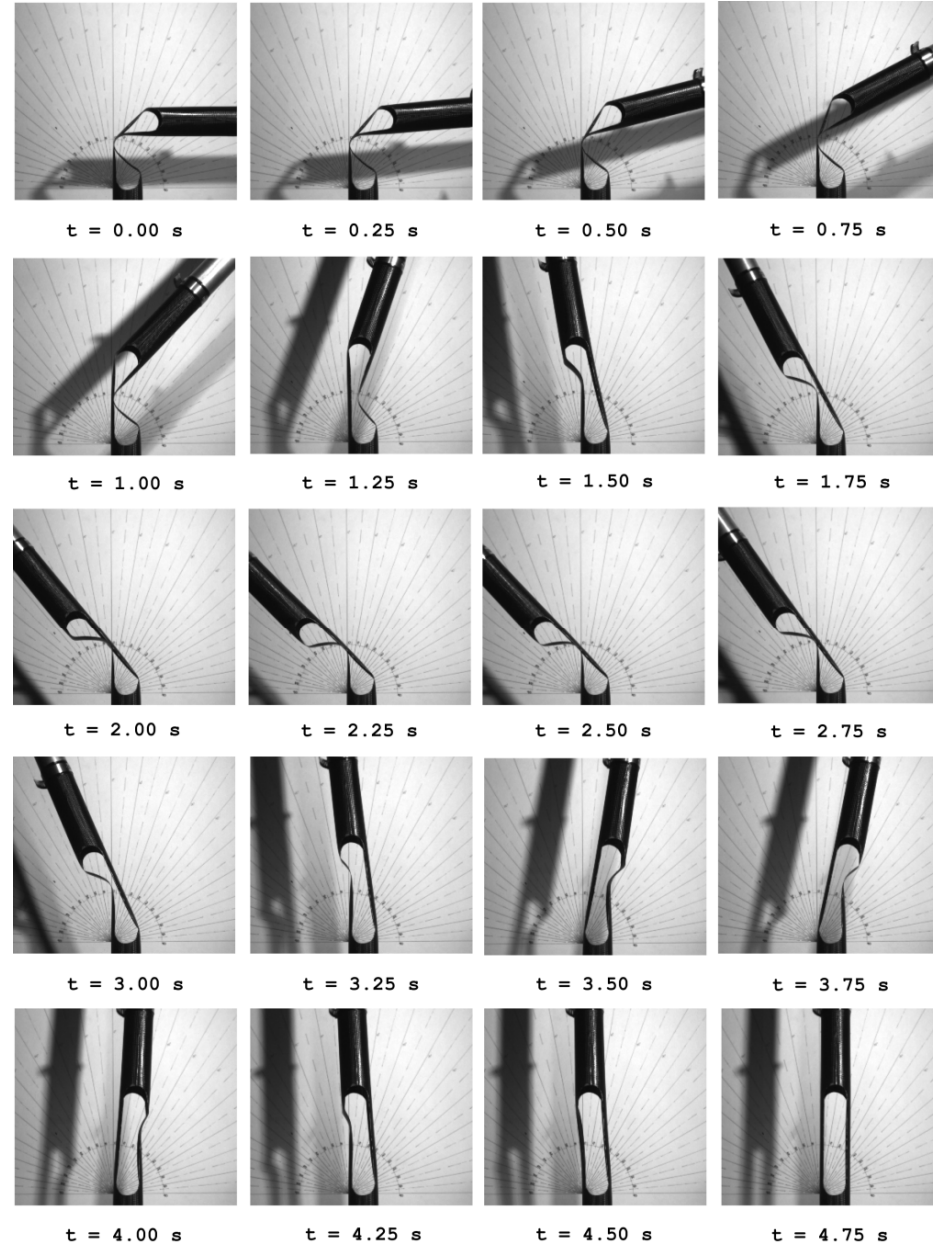
- Deployment phase: 1.45 s
- Buckling phase: 2.96 s
Maximum overshoot 45 deg
- Vibration phase: 20 s
2 deg amplitude, period 0.2 s



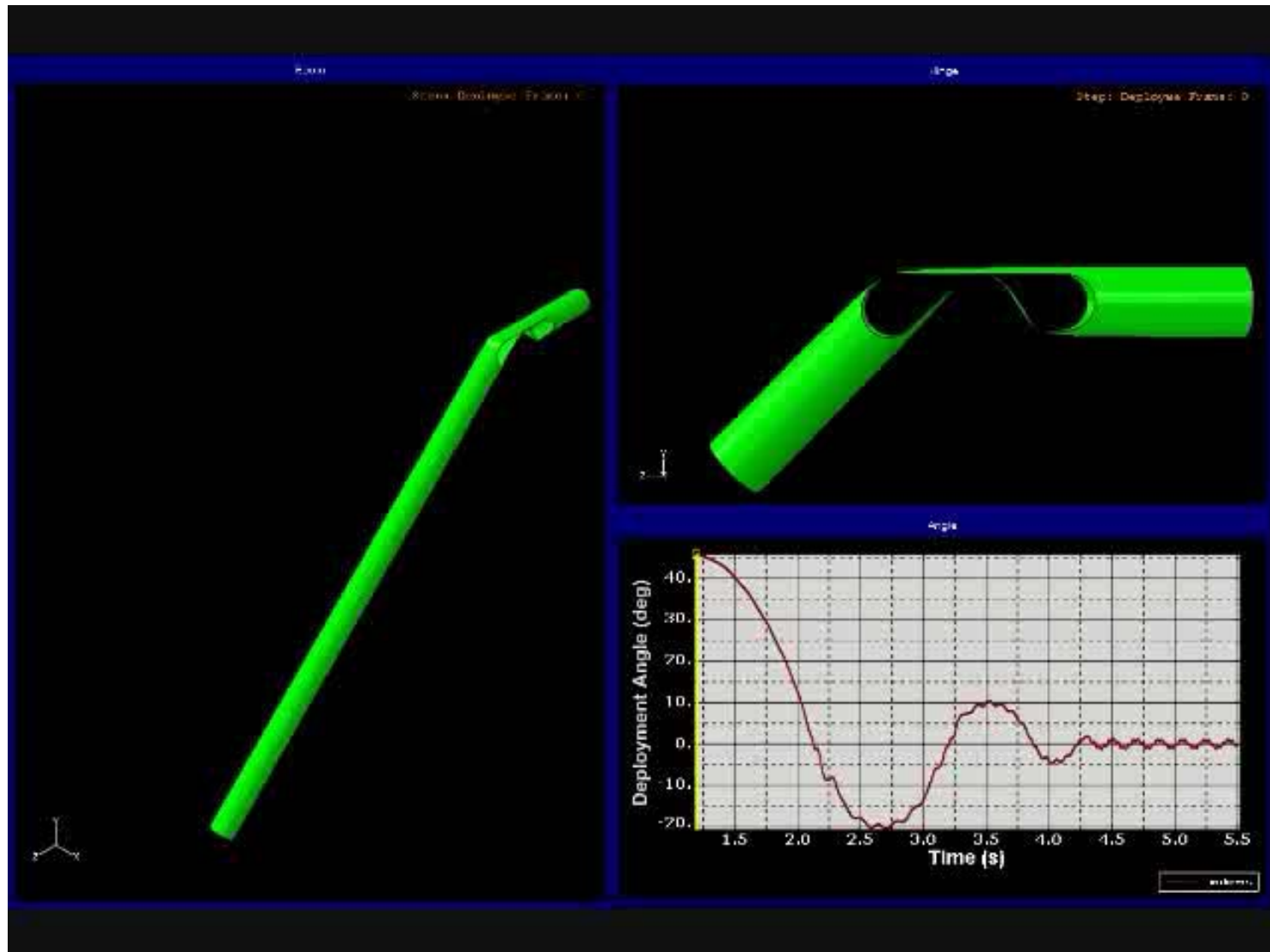
Angle vs Time



- Deployment phase: 1.45 s
- Buckling phase: 2.96 s
Maximum overshoot 45 deg
- Vibration phase: 20 s
2 deg amplitude, period 0.2 s

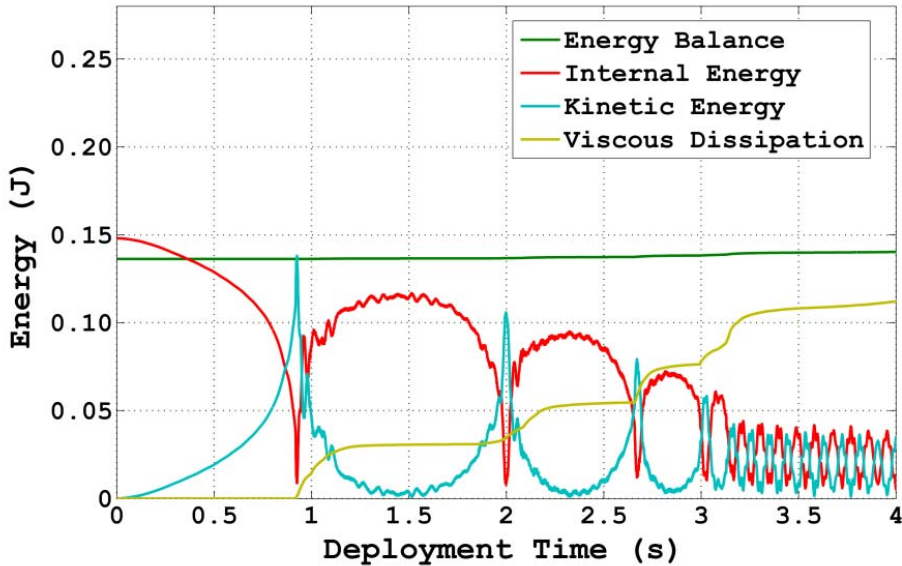


Deployment Simulation (45 deg)

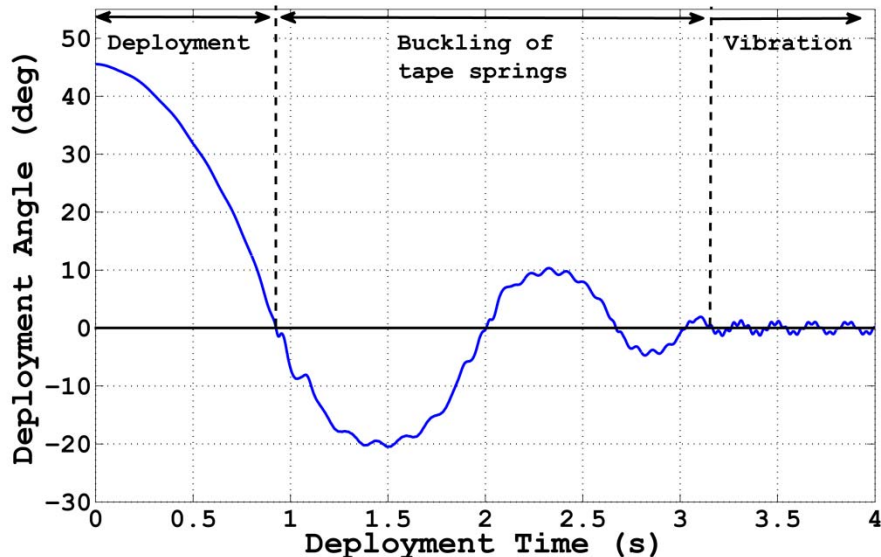


Simulation time is real time. No damping in simulation.

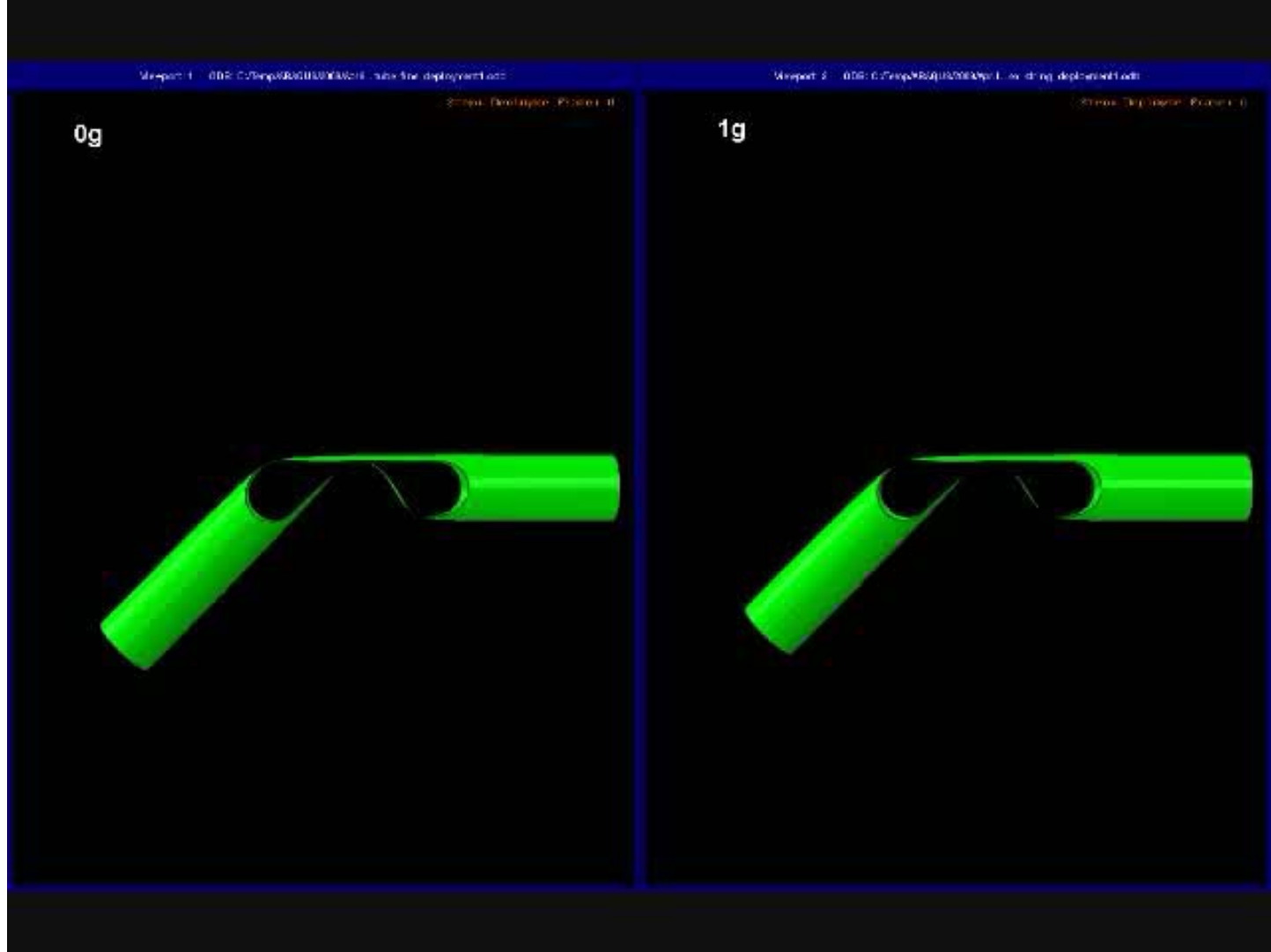
Simulation Results (45 deg)



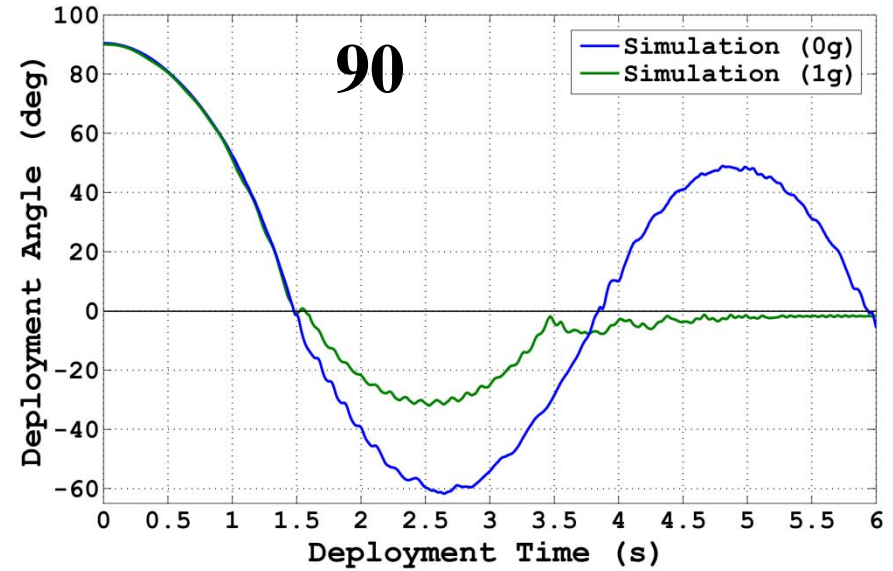
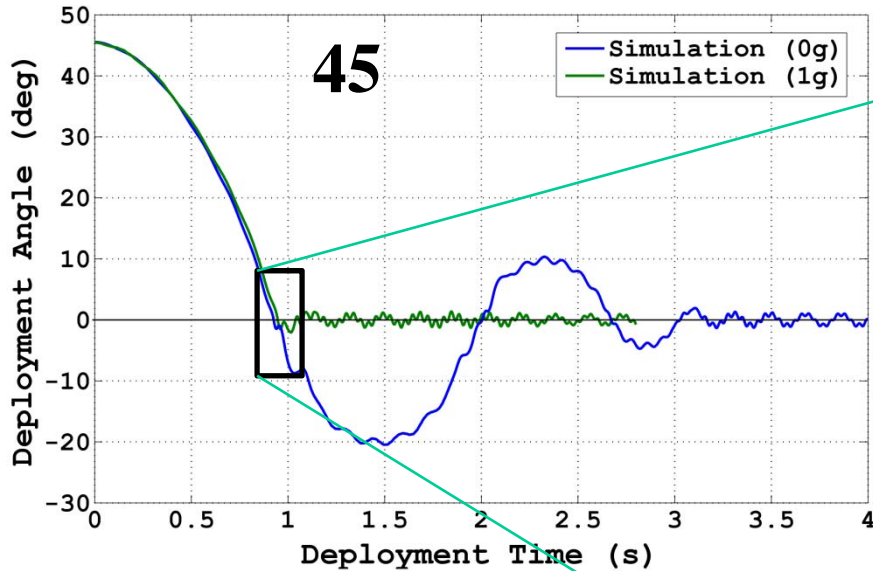
- Constant energy balance
- Most energy dissipation occurs when tape springs buckle
- Deployment phase: 0.93 s
- Buckling phase: 2.24 s
 - Max. overshoot 20.5 deg
- Vibration phase:
 - Amplitude = 1 deg
 - Period = 0.18 s



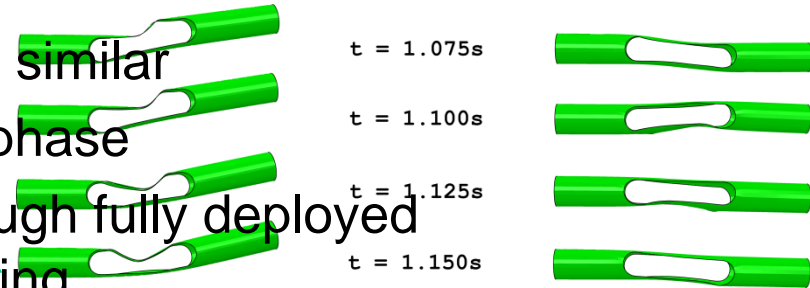
0-g vs. 1-g Deployment



0-g vs. 1-g Deployment

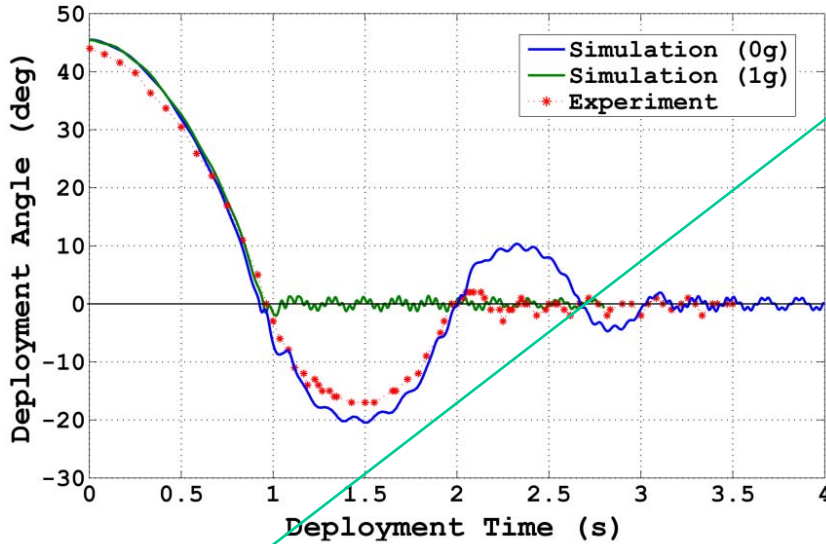


- Deployment and vibration phases are similar
- Significant differences in the second phase
 - Zero-gravity simulation goes through fully deployed configuration 4 times before latching
 - Simulation with gravity offload system latches fully the first time

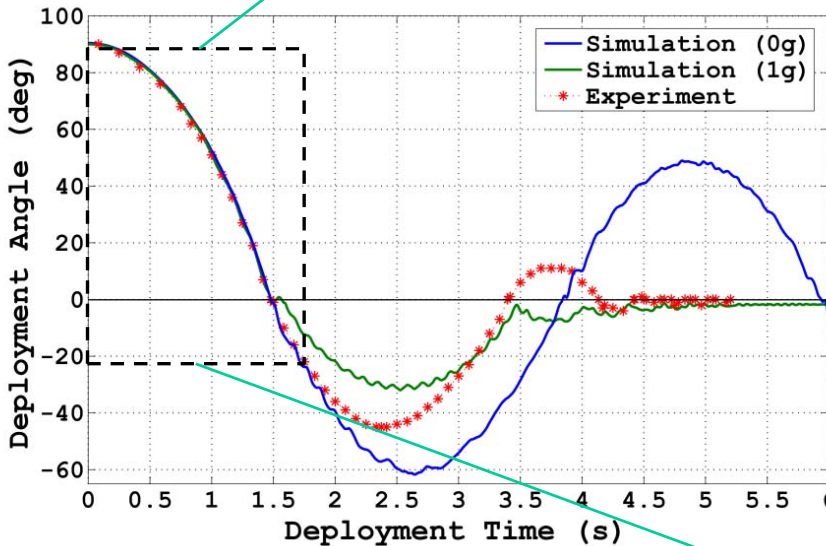


Comparison with Experiments

45

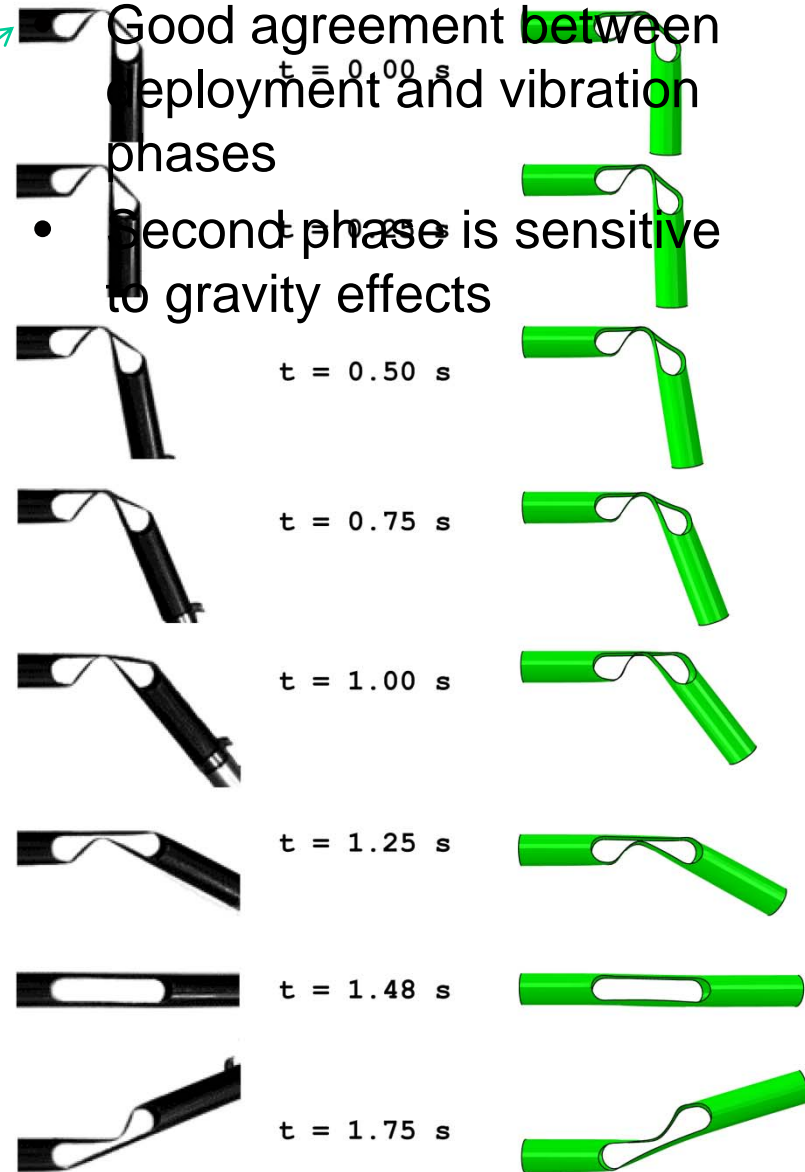


90

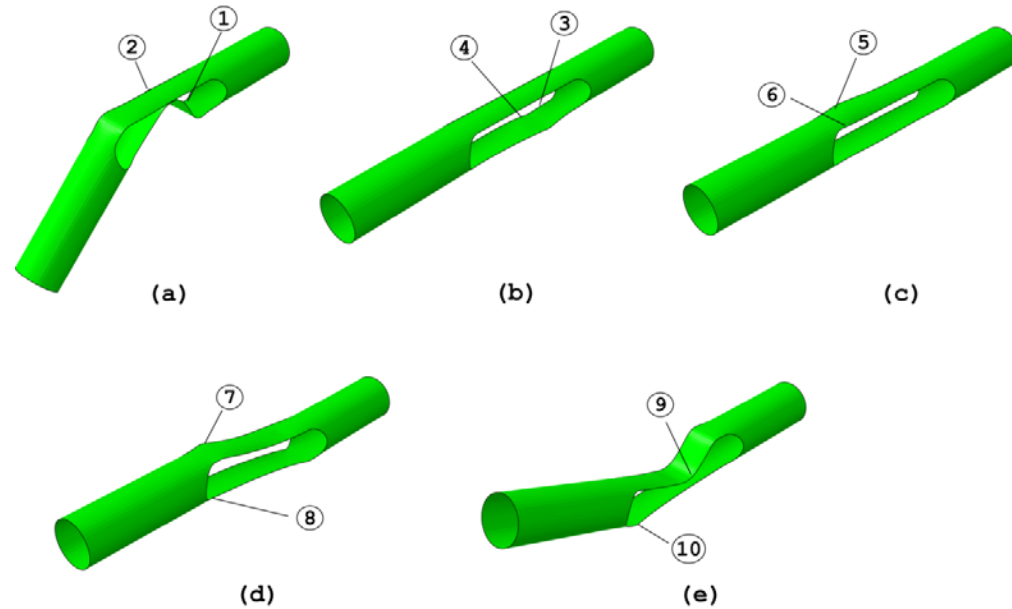


Good agreement between deployment and vibration phases

- Second phase is sensitive to gravity effects



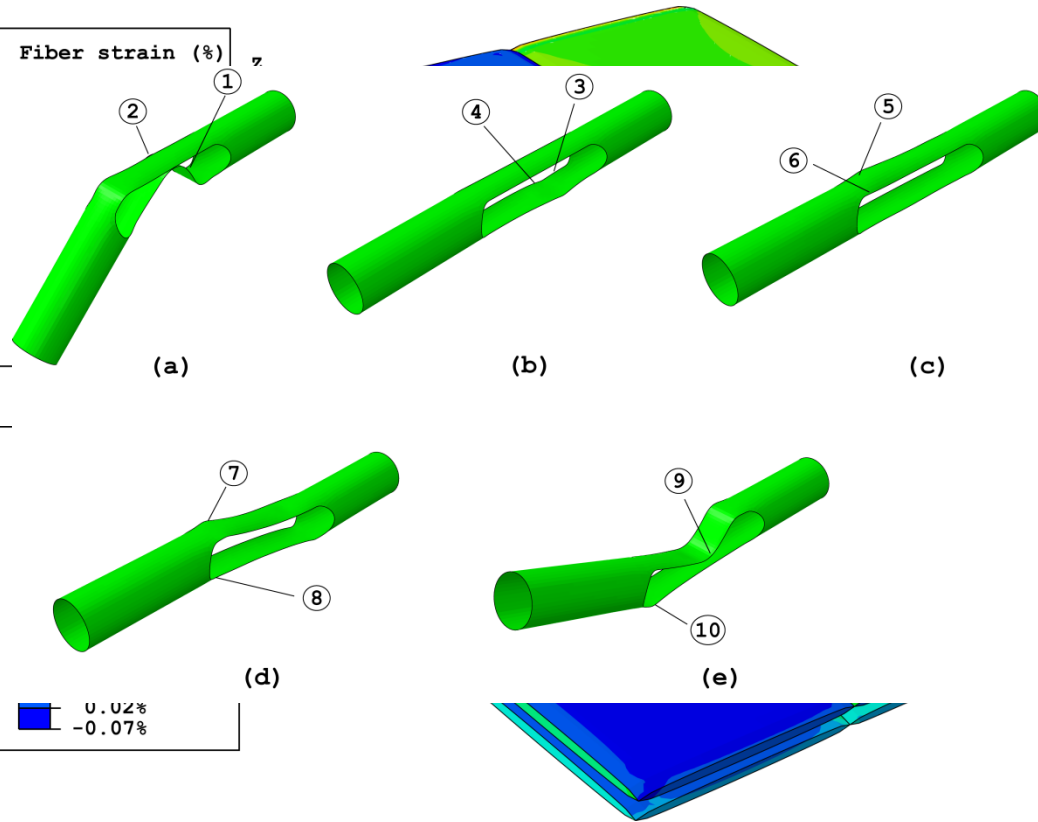
Given a Hinge Design, is it Safe?



- (a) Fully folded
- (b) Just before snap-back
- (c) Snap-back
- (d) Back buckling
- (e) Maximum overshoot

- Based on maximum absolute value of mid-plane strains along the fibre
 - 5 critical configurations
 - 2 critical locations for each
- Strains and curvature components with respect to fibre directions are inserted into unit cell model

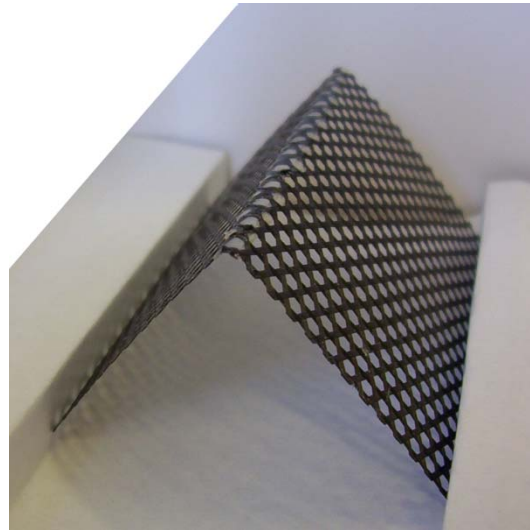
Failure Analysis



- Separate periodic unit cell analysis for each location
- Longitudinal strains are taken by fibers
- Transverse strains are taken by matrix
- Ultimate tensile strain of T300-1k fibers = 1.5%
- Ultimate tensile strain of Hexply 913 resin $\approx 1.93\%$

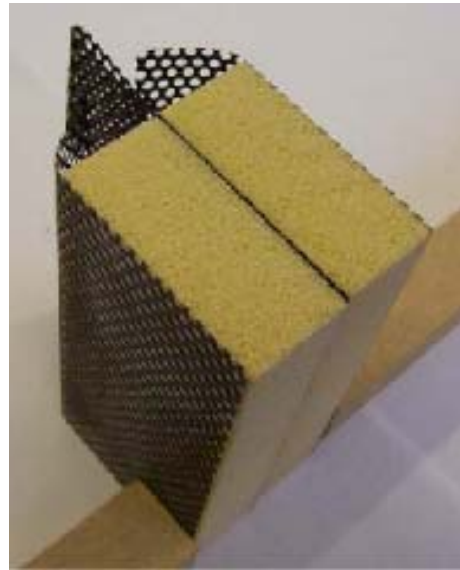
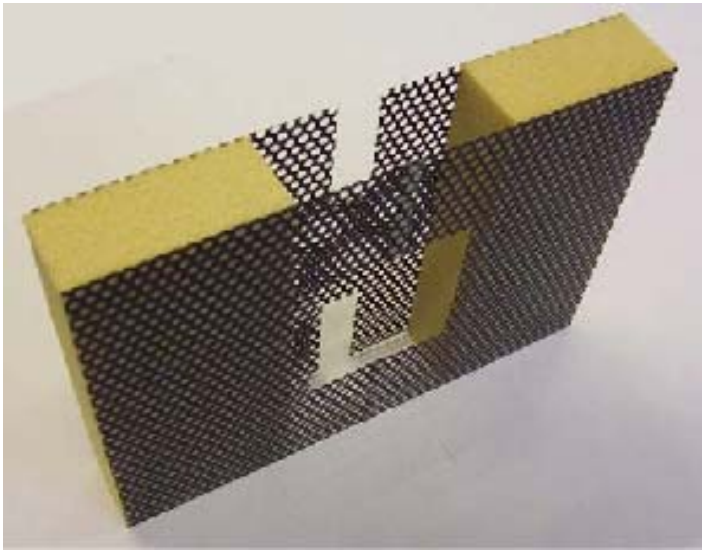
Location	1	Location	1	6	7	8	9	10
Fibre strain (%)	0.42	Fibre strain (%)	0.42	-0.60	0.42	-0.94	0.61	0.13
Matrix strain (%)	0.92	Matrix strain (%)	0.92	-1.46	1.10	-2.00	1.30	-1.86

Carbon Fibre Reinforced Silicone Hinges



- Particularly interesting for sharp creases
- Does it recover fully?

Offers interesting possibilities



Bibliography

- Aoki, T. & Yoshida, K. (2006) Mechanical and thermal behaviors of triaxially-woven carbon/epoxy fabric composite. *47th Structures, Structural Dynamics and Materials Conference, AIAA-2006-1688*
- Daniel, I.M. and Ishai, O. (2005) *Engineering Mechanics of Composite Materials*, Oxford University Press, New York, Second Ed.
- Karkainen, R. L. & Sankar, B. (2006) A direct micromechanics methods for analysis of failure initiation of plain weave textile composites. *Composites Science and Technology, 66, 137-150.*
- Kueh, A.B.H., and Pellegrino, S. (2007) *Triaxial weave fabric composites. Department of Engineering, University of Cambridge, Technical Report CUED/D-STRUCT/TR223.*
- Kueh, A. & Pellegrino, S. (2009) Computation and validation of constitutive matrix of single-ply triaxial weave fabric composites *Submitted for publication.*
- Mallikarachchi, H. M. Y. C. & Pellegrino, S. (2009) Deployment dynamics of composite booms with integral slotted hinges. *50th Structures, Structural Dynamics and Materials Conference, AIAA-2009-2631*
- Mallikarachchi, H. M. Y. C. & Pellegrino, S. (2009) Quasi-static folding and deployment of ultra-thin composite structures. *Submitted for publication.*

Acknowledgments

- Ahmed Kueh
- Chinthaka Mallikarachchi
- Jeffrey Yee
- Phil Howard at EADS Astrium
- Hexcel
- Julian Santiago-Prowald at ESA
- Northrop Grumman